



MAURITIUS RESEARCH COUNCIL

ADAPTIVE CODING TECHNIQUES FOR TIME VARYING CHANNELS

Final Report

Year 1998

MAURITIUS RESEARCH COUNCIL

Address:

Level 6, Ebène Heights,
34, Cybercity,
Ebène 72201,
Mauritius.

Telephone: (230) 465 1235
Fax: (230) 465 1239
Email: mrc@intnet.mu
Website: www.mrc.org.mu

This report is based on work supported by the Mauritius Research Council under award number MRC/RUN-9713. Any opinions, findings, recommendations and conclusions expressed herein are the author's and do not necessarily reflect those of the Council.

MONITORING UNIT REPORT

TITLE: ADAPTIVE CODING TECHNIQUES FOR TIME VARYING CHANNELS

PI: MR K. M. S. SOYJAUDAH

MEETING NO.	:	1	DATE:	29/9/97
LOCATION	:	UOM	DURATION:	30 MINS
PRESENT	:	MR K. M. S. SOYJAUDAH		

RESEARCH OBJECTIVES:

To establish a multimedia radiolink between University of Mauritius and Lancaster University.

To use this link to test performance of adaptive encoding/decoding algorithms proposed.

To enhance research activities in the field of communication at the University of Mauritius and to promote further research collaboration with Lancaster University

To use this link to communicate with neighbouring islands.

To use this radiolink for transmission of weather news independently by the Mauritius meteorological services during cyclonic conditions.

WORK COMPLETED:

- A paper was presented at the 4th International Symposium on communication theory and applications on embedded coding techniques.
- The antenna, receiver, and software have been set up. Data is being received from Norway.

OUTSTANDING WORK:

- Data received from Norway must be analysed by Defence Research Agency UK (DRA) in order to proceed with the research

PROBLEMS ENCOUNTERED BY PI:

- The main problem at the beginning of the project was that Telecoms authority only gave clearance for transmission after the receiver was taken on loan from Defence Research Agency UK.

REQUESTS/ SUGGESTIONS FROM RESEARCH TEAM:

Although not budgeted originally, a computer would be needed to be able to fit all the expansion and aids needed to complete the project.

The budget earmarked for Antenna has not been asked. This can be reallocated for a PC.

REQUESTS/ SUGGESTIONS TO PI:

IN CORRESPONDENCE:

- PI to submit copy of paper presented to 4th PI to submit a more complete report on work completed as at 30 September 1997.
- Next progress report due March 1998.
- Final report due June 1998.

DIFFUSION OF FINDINGS

In view of the liberalisation of telecommunication beyond year 2000, this project could be the basis for setting up a commercial exploitation this time for voice and data transmission.

MONITORING TEAMS COMMENTS:

Adaptive Coding Techniques for Time Varying Channels

by

K.M.S Soyjaudah

A Report submitted to MRC

July 1998

Contents

List of Figures and Tables

Acknowledgements

Abstract

List of Symbols

List of Abbreviations

Chapter 1	Introduction	1
1.1	Introduction	1
1.2	Review of Error Protection Techniques for Time Varying Channels	1
1.3	Channel Models	4
1.3.1	Discrete Memoryless Channel	4
1.3.2	Channel with Memory	5
1.4	Organisation of the report	7
Chapter 2	Channel Coding and Modulation Techniques	9
2.1	Introduction	9
2.2	Convolutional Codes	9
2.2.1	State Representation and State Diagram	13
2.2.2	The Tree Diagram	13
2.2.3	The Trellis Diagram	15
2.3	Block Codes	15
2.3.1	Array Codes	19
2.3.2	Single Parity Check Code	20
2.3.3	Row and Column Array Codes	20
2.3.4	Diagonals Checks Array Codes	24
2.3.5	Folded Diagonal Checks Array Codes	25
2.3.6	Multidimensional Array Codes	26
2.4	Generalised Array Codes	26
2.4.1	GAC Code Construction	26
2.4.2	Design of (8,4, 4) and (7,4,3) Codes	28
2.4.3	Design of (15,7,5) Code	29
2.5	Modified Trellis Design Technique Proposed	29
2.6	Low Complexity Trellis Decoding of Linear Block Codes	32
2.6.1	Trellis Design Procedure of Linear Block Codes	32
2.6.2	Trellis Diagrams of the (8,4,4) GAC and (7,4,3) Hamming codes	34
2.6.3	Trellis structure of the (9,6,3) GAC Code	35

Chapter 3: Embedded Coding Technique using Linear Block Codes	37
3.1 Introduction	37
3.2 Embedded Code Encoding/Decoding Procedures	39
3.2.1 Modified Embedded Array Code	40
3.2.2 Embedded Convolutional Code	41
3.3 Embedded Code employing Linear Block Code and Trellis Decoding	43
3.3.1 The Overall System	44
3.3.2 Embedded Code Encoding Procedures	45
3.3.3 The Decoder	47
3.4 Simulation Results and Discussions	50
3.5 Modified Embedded Code employing Linear Block Codes	53
3.5.1 The Decoder	54
3.5.2 Statistical Channel Evaluation employing the Trellis of the Linear Block Codes	55
3.6 Simulation Results and Discussions	59
3.7 Embedded Code employing Linear Block Codes and Nested Trellis Decoding	62
3.8 Simulation Results and Discussions	64
Chapter 4 Trans-equatorial Link Between Mauritius and Europe	68
4.1 Introduction	68
4.2 Measurement System	68
4.3 Transmit system configuration	71
4.4 Receive station configuration	73
4.5 Time of flight search mode	76
4.6 Delay Doppler measurement mode	76
4.7 Results and discussions	81
Chapter 5 Conclusion and Further Work	191
5.1 Summary	191
5.2 Discussions	191
5.3 Further work	193
Bibliography	195

List of Figures and Tables

Fig. 1.1 Gilbert model of channel with memory	5
Fig 2.1 Convolutional (2,1,2) encoder	9
Fig. 2.2 State diagram of the (2,1,2) convolutional encoder	11
Fig. 2.3 Tree diagram for the (2,1,2) convolutional encoder	13
Fig. 2.4 Trellis diagram of the (2,1,2) convolutional encoder	14
Fig. 2.5 Structure of an RAC array code	20
Fig. 2.6 Diagonal check on an information array	23
Fig. 2.8 Trellis diagram of (3,2,2)(4,3,2) code as per previous scheme (incorrect)	31
Fig. 2.9 Trellis structure of the (8,4,4) GAC code	34
Fig. 2.10 Trellis structure of the (7,4,3) Hamming code	34
Fig. 3.1 Structure of an embedded code	39
Fig. 3.2 (64,23) Modified embedded array code block structure	41
Fig. 3.3 Embedded convolutional code block structure	42
Fig. 3.4 ARQ protocol of the embedded code	43
Fig. 3.5 System block diagram	45
Fig..3.6 Structure of embedded code employing linear block codes	46
Fig.3.7 Trellis diagram of the (16,5,8) GAC code	48
Fig. 3.8 Trellis diagram of the (16,9,4) RAC code	48
Fig. 3.9 Trellis diagram of the (16,11,4) GAC code	49
Fig. 3.10 BER vs SNR for components of embedded code	51

Fig. 3.11 Output BER vs Channel BER for embedded and (65,48,4) RAC code	52
Fig. 3.12 Throughput vs Channel BER for Embedded and (65,48,4) codes	52
Fig. 3.13 Throughput vs SNR for Embedded and (65,48,4) codes	53
Fig. 3.14 Structure of the modified embedded code employing linear block codes	53
Fig. 3.15(i) PDF vs Mean error detection metric of the (16,5,8) GAC code	57
Fig. 3.15(ii) PDF vs mean error detection metric for the (16,11,4) GAC code	57
Fig. 3.16(i) Mean error detection metric vs SNR for the (16,5,8) GAC code	58
Fig. 3.16(ii) Mean error detection metric and its standard deviation for the (16,11,4) GAC code	58
Fig. 3.17 Output BER vs Channel BER for embedded code and (16,11,4) GAC code	60
Fig. 3.18 Throughput vs Channel Bit Error Rate for embedded code and (16,11,4) GAC code	60
Fig. 3.19 Throughput vs SNR for embedded and (16,11,4) GAC code	61
Fig. 3.20. Structure of embedded code based on GAC codes	63
Fig. 3.21 Nested trellis of (32,6,16), (16,5,8) and (8,4,4) GAC codes	64
Fig. 3.22 Output BER vs SNR	66
Fig. 3.23 Output BER vs Channel BER	66
Fig. 3.24 Throughput vs Channel BER	67

Fig. 3.25 Throughput vs SNR	67
Fig.4.1 Configuration of Transmit System	72
Fig.4.2 Receive Station Configuration	74
Fig.4.3 Location of the HF receive antenna	75
Fig.4.4 HF receive antenna	75
Fig.4.5 Transmitted Waveform Frame Structure in Delay Doppler (DD) Measurements Mode	77
Fig.4.6 -Calculation of Doppler Spectra for Each Time Delay Interval Using Doppler Integration	78
Fig. 4.7 Data received from transmitter in Scandinavia situated at 70.0° North and 5.0° East.	81
Fig. 4.8 Data from Guildford transmitting at a frequency of 18.188 MHz	82
Fig. 4.9 Data from Guildford transmitting at a frequency of 20.2125 MHz	82
Fig. 4.10 Data from Guildford transmitting at a frequency of 23.7595 MHz	82
Table.4.1 - Trade-offs between Delay Range, Doppler Range/Resolution and total DD Measurement Time (3 kHz bandwidth and 9600 samples per second)	80

Acknowledgements

I wish to express my sincere gratitude and thanks to MRC ,UOM and DRA ,UK for funding the project. My thanks also goes to Prof. B. Honary of Lancaster University, UK and to Mel Maundrell, Nigel Davies, Bob Bagwell of DRA UK for their technical assistance in making the HF link work and for transmitting the signals to be measured. I would also like to acknowledge the support and help of the technical staff of the Electrical and Electronic Engineering, UOM especially Paul Leung Kam Tsang and H. Woomchurn.

Abstract

Adaptive coding techniques for time varying channels such as the HF (2-30) MHz have been under investigation for several decades [Honary 1981, Katakol 1987, Zolghadr 1989, Bate 1992, etc.]. Forward error correction applied to these channels are designed to give the desired performance for the worst channel state. Hence when the channel is relatively error free unnecessary error correction power and redundancy is being employed. This naturally reduces the overall information rate. In order to transmit data efficiently in a time varying channel an ideal error control scheme should achieve a lower average output bit error rate than that obtainable with a fixed rate system. This is done by matching the code to the changing channel conditions.

In this report a number of embedded coding techniques employing block codes for time varying channels have been proposed and investigated. A novel statistical channel evaluation technique based on the trellis of block codes has also been devised. The HF link has been established with a receiver station in Mauritius and measurement of data from UK has shown that it is working as expected.

List of Symbols

$A(t)$	time varying amplitude
C	channel capacity
$E(R)$	positive function of R
e	error vector
f	frequency
$g^{(i)}$	generator sequence i
G	generator matrix
G_a	asymptotic coding gain
H	parity check matrix
k	number of information bits
k_1	number of information bits in a row of an RAC code
k_2	number on information bits in a column of an RAC code
n	number of bits in codeword
n_1	number of rows in RAC code
n_2	number of columns in RAC code

N_c	trellis depth
N_s	number of states in trellis
N_{symbols}	number of symbols per codeword
p	bit error probability
$p(j i)$	probability of receiving j given that i was transmitted
$P(E)$	error probability
R	transmission rate
s	syndrome of received vector
s_i	i^{th} signal
$S(t)$	carrier wave
T	symbol duration
U	information row vector
V	output vector
X	received vector
$\theta(t)$	time varying angle
ω	radian frequency of the carrier
$\phi(t)$	time dependent phase

List of Abbreviations

ARQ	Automatic Repeat Request
AWGN	Additive White Gaussian Noise
BSC	Binary Symmetric Channel
GAC	Generalised Array Code
FEC	Forward Error Correction
FEC/FED	Forward Error Correction/Forward Error Detection
HF	High Frequency
MB	Meteor Burst
MFSK	Multi-Frequency Shift Keying
RAC	Row and Column
RM	Reed Muller

Chapter 1

Introduction

1.1 Introduction

Over the past few decades, there has been increasing demand for efficient and reliable digital data transmission and storage systems. One of the major difficulties in the design of such communication systems is the control of errors in the noisy channel. Proper channel error control technique can reduce the bit error rate to a reliable low value. This was shown in a landmark paper in 1948 by Shannon [Shannon 1948] and is the most important and striking result on the transmission of information over a noisy channel. The theorem is known as the Shannon's Coding Theorem and states that for every channel there is a definite maximum transmission rate called the channel capacity, denoted by C , and that for any transmission rate, R less than C , there exist codes with maximum likelihood decoding, having an arbitrarily small error probability $P(E)$. In other words for any given rate $R < C$ and length n , there exists a code such that the probability of erroneous decoding is given by

$$P(E) \leq e^{-nE(R)}$$

where $E(R)$ is a positive function of R for $R < C$ and is specified by channel transition probabilities. Unfortunately Shannon's theorem only shows the existence of efficient error control codes, but does not indicate how these codes are constructed. Hence we have the problem of searching for good codes with large n in order to achieve Shannon's limit.

1.2 Review of Adaptive Error Coding techniques

Time varying or fading channels, for example, the High Frequency (HF 2-30 MHz) and the Meteor Burst (MB) have been under study ever since the beginning of Electronic Communications. These channels, because of their time and frequency dependent nature, have caused the greatest challenge to the designers of

communication systems. Earliest methods to tackle the problems associated with such channels were the different types of linear diversity combining techniques [Brennan 1959]. Other schemes that have been suggested to overcome fading and noise are the adaptive schemes wherein power and transmission rate can be varied according to the channel conditions. This is monitored at the receiver and the information is fed back to the transmitter through a low capacity feedback channel [Hentinen 1974, Hancock and Lindsay 1963, Cavers 1972]. The adaptation of power and transmission rate can be done independently or in a combined way. Another way to combat these difficulties is to use error protection technique. Two schemes are used, namely (i) FEC (Forward Error Correction) and (ii) ARQ (Automatic Repeat Request).

FEC systems can correct a mixture of burst and random errors and are most suitable for predictable channels, for example, the satellite channels. Owing to the time varying nature of the HF/MB channels fixed rate error correcting codes provide unnecessary correction power much of the time, that is, when the channel is relatively error free. This increases the redundancy being used and reduces the throughput efficiency [Bate 1992, Honary, Darnell and Vongas 1993]. Honary et al. [Honary 1981, Honary and Farrell 1985] have designed FEC for time varying channels to operate over most of the range of the channel capacities encountered, but by varying the information rate in order to obtain improved information rate without any significant deterioration of the overall sink error rate.

ARQ systems depend on feedback information received from the receiver to indicate the state of the received message. These systems employ a relatively low “overhead of check bits” for reliable error detection [Goodman 1975]. It has been shown that a properly designed system of this type is very reliable [Lin, Costello and Miller 1984]

but under poor channel conditions the number of repetitions required may be excessive. A combination of FEC with retransmission error control can improve the performance of the system. This scheme is known as hybrid ARQ. The correct choice of correction power can significantly increase the reliability and the throughput efficiency by reducing the number of retransmission required [Goodman 1975].

To tailor the code more closely to the state of the channel, adaptive techniques with variable redundancy [Goodman 1975] are used. An adaptive coding scheme varies the amount of redundancy according to the state of the channel and so increases the overall transmission rate. An efficient adaptive error control scheme should achieve a lower average output bit error rate with a higher throughput efficiency than that obtainable with a fixed rate system. This is achieved by matching the code to the changing channel conditions. At the receiver, some means of evaluating the state of the channel is required in order to vary the coding scheme. The receiver measures the state of the channel and based on it decides the adaptation strategy. It then sends this information to the transmitter. Madelbaum [Madelbaum 1974] has proposed an incremental redundancy adaptive scheme in which the number of check bits sent is varied as the channel state changes. Katakol [Katakol 1987] has shown that adaptive coded variable rate systems give considerable improvement over other type of adaptive systems. It is also possible to vary the transmission rate, either without modifying the code rate or combining both techniques by using embedded techniques [Darnell et al. 1988, Zolghadr et al. 1988, Darnell et al. 1989, Zolghadr 1989]. Bate [Bate 1992] has (i) investigated on the recommendations of Goodman [Goodman 1975], burst and random error correcting product codes (ii) investigated the effects of interleaving on adaptive convolutional codes and (iii) introduced an embedded Reed-

Solomon code in which new information can be sent simultaneously with repeated information. In this report a number of embedded coding techniques employing block codes for time varying channels have been proposed and investigated. A novel method of statistical channel evaluation technique based on the trellis of block codes has been devised. The purposes of setting up the link between Europe and Mauritius is described and the early results are presented.

1.3 Channel Models

Channels can be classified as (a) discrete memoryless channels and (b) channels with memory. Although real channels are a combination of both, usually one is dominant.

1.3.1 Discrete Memoryless Channel

A discrete memoryless channel is characterised by a discrete input alphabet, a discrete output alphabet, and a set of conditional probabilities, $p(j|i)$ ($1 \leq i \leq M, 1 \leq j \leq Q$)

where i represents a modular M -ary input symbol, j represents a demodulator Q -ary output symbol and $p(j|i)$ is the probability of receiving j given that i was transmitted [Sklar 1988]. Each output symbol depends only on the corresponding input symbol. In this channel transmission errors occur independently in digits positions, i.e. each transmitted digit is affected independently by noise. A special case of the DMC is the Binary Symmetric Channel in which the input and output alphabet sets consist of binary elements (0 and 1). The transition probabilities are symmetric and are given by

$$p(0|1) = p(1|0) = p \quad 1.1$$

$$p(1|1)=p(0|0)=1-p$$

1.2

This means that the probability of receiving a transmitted symbol in error is p and that of receiving it correctly is $1-p$.

1.3.2 Channel with Memory

For channels with memory, the occurrence of an error increases the probability of a further error. In this manner errors tend to cluster into bursts. A simple representation of channels with memory is the Gilbert model[Gilbert 1960] shown in Fig. 1.1

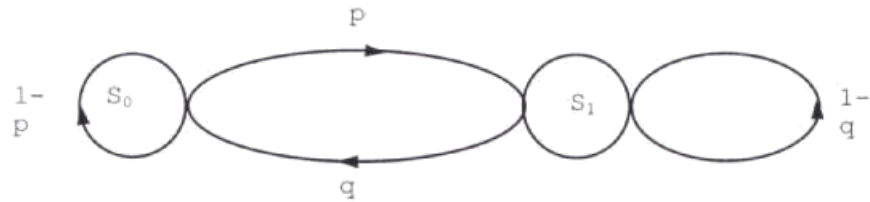


Fig. 1.1 Gilbert model of channel with memory

This model is described by the transition probabilities [Zolghadr et al. 1989, Kanai and Sastry 1978] as

$$p(S_0|S_1) = q$$

1.3

$$p(S_1|S_0) = p$$

1.4

and

$$p(S_1) = \frac{p}{p + q} \quad 1.5$$

$$p(S_0) = \frac{q}{p + q} \quad 1.6$$

The Gilbert model consists of a good state S_0 and a bad state S_1 . No errors are produced in the good state while error bursts are generated in the bad state. Also the capacity of the Gilbert channel is higher than that of the DMC. Examples of channel with memory are telephone lines, HF radio and troposcatter links. These can be regarded as channels in which there are extended time intervals displaying a relatively low random error rate, separated by error bursts with much higher error rate. Memory in a real communication channel arises due to effects like intersymbol interference caused by filtering, fading caused by ionospheric reflections among others. Error correcting codes designed to correct random errors are not efficient for correcting burst errors. Codes specifically designed for correcting burst errors are used to deal with burst errors.

1.4 Organisation of the Report

The second chapter of the report discusses some background theory necessary for understanding the rest of the thesis.

In chapter three the embedded encoding technique is described. Then an embedded encoding scheme for time varying channels (i) employing GAC and RAC array codes and inner codes for error correction and outer codes for error detection/channel evaluation is introduced, and (ii) new structures of embedded coding employing RAC and GAC codes but without any outer code is introduced. The error detection or statistical channel evaluation process employing the trellis of GAC is explained. The

simulation results showing the improvement provided by the embedded codes over an RAC code of same block size as the embedded code in case (i) and over a component code in case (ii) are emphasised. Finally a new embedded code that does not involve any outer code and does the decoding of the component codes with a single trellis but in a nested fashion is introduced and analysed.

Chapter four describes the purpose of setting the HF link between Europe and Mauritius, the system employed to measure multipath dispersion, Doppler spread and Doppler shift on multi-mechanism communication channels and the early results obtained.

Chapter concludes the work carried out so far and gives suggestion for further work in this area.

Chapter 2

Channel Coding Techniques

2.1 Introduction

Channel coding can be divided into waveform coding and structured sequences. In waveform coding the waveforms are transformed such that they are less prone to errors. Structured sequences, on the other hand, deal with the process of adding redundant bits to the data sequences that can subsequently be used for error detection and error correction. Both processes give rise to coded signals with better distance properties and hence better performance than their uncoded counterparts. Error control coding which is considered in the following sections can be classified broadly as convolutional and block coding.

2.2 Convolutional Codes

A convolutional code is described by three integers n , k and m as (n,k,m) where k is the number of inputs to the encoder, n is the number of outputs from the encoder and m is the number of shift registers in the encoder. Unlike in the case of block codes, in convolutional codes, n does not describe a block or codeword length. The constraint length is given by $n(m+1)$ and it controls the redundancy in the code. Since each information bit remains in the encoder for up to $m+1$ time units, and during each time unit can affect any of the n encoder outputs the constraint length is interpreted as the

maximum number of encoder outputs that can be affected by a single information bit.

The code rate of a convolutional code is $\frac{k}{n}$. However for information sequence of

finite length kL , the corresponding codeword has length $n(L+m)$ and the code rate is

given by $\frac{kL}{n(L+m)}$ [Lin and Costello 1983]. A convolutional code is characterised by a

generator matrix G such that G readily converts a given input row vector U into an

output vector V as shown in equation 2.1.

$$V=U.G$$

2.1

Obviously G is different from that of a linear block code case since it is a semi-infinite

matrix in the convolutional case. Fig. 2.1 shows a $(n,k,m) = (2,1,2)$ convolutional

encoder.

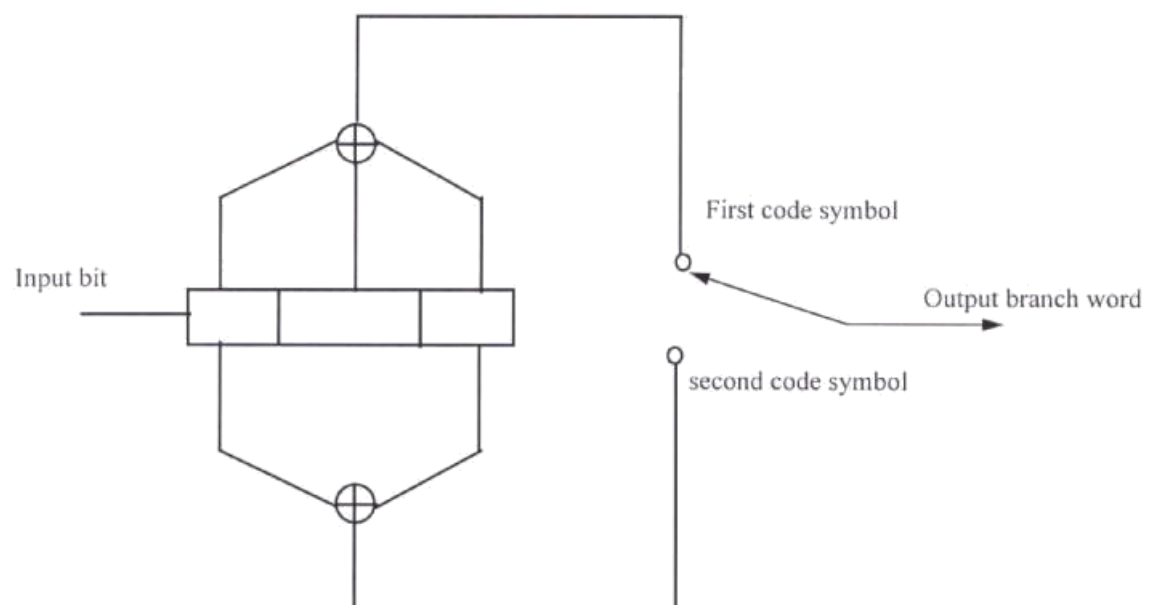


Fig 2.1 Convolutional (2,1,2) encoder

This encoder is described as a (2,1,2) encoder since there are two modulo-2 adders, and has a constraint length 6 and a code rate $\frac{k}{n} = \frac{1}{2}$. At each input bit time, a bit is shifted into the leftmost stage and the bits in the register are shifted one position to the right. The output switch then samples out the output upper and then that of the lower modulo-2 adders. The sampling is repeated for each of the inputted bit. If the encoder input is an impulse given by

$$U = (100.....)$$

the impulse responses of the two branches are respectively

$$V^{(1)} = (10100..)$$

and

$$V^{(2)} = (11100..)$$

These impulse responses are called generator sequences and are denoted by

$$g^{(1)} = V^{(1)} \text{ and } g^{(2)} = V^{(2)}.$$

For any given encoder input U , the two outputs $V^{(i)}$ $i=1,2$, can be found by discrete time convolution for all time instant $m \geq 1$ as [Gibson 1989]

$$V^{(i)} = U * g^{(i)} = \sum_{j=0}^{v-1} U_{m-j} g_{j+1}^{(i)} \quad 2.2$$

$$V^{(i)} = U_m g_1^{(i)} + U_{m-1} g_2^{(i)} + \dots + U_{m-v+1} g_v^{(i)} \quad 2.3$$

with $U_{m-j} = 0$ for $m-j \leq 0$. The encoder output sequence is given by

$$V = (V_1^{(1)} V_1^{(2)} V_2^{(1)} V_2^{(2)} V_3^{(1)} V_3^{(2)} \dots) \quad 2.4$$

The generator matrix of the convolutional codes can be obtained by interleaving the generator sequences to form a row and then creating subsequent rows by shifting n

2.2.1 State Representation and State Diagram

Simple encoders may be represented with a state diagram where each state is defined as the contents of the rightmost m stages of the convolutional encoder. Fig. 2.2 shows the state diagram of the (2,1,2) convolutional encoder. The states of the register are designated 00, 10, 01 and 11. Only two transitions can emanate from each state. Each branch is labelled with two values, input/output. From each state it is only possible to move into two possible states.

2.2.2 The Tree Diagram

The tree diagram by adding the dimension of time to the state diagram makes it easier for tracking the encoder transitions. The tree diagram for the (2,1,2) convolutional encoder is given in Fig. 2.3. Although the tree diagram allows one to dynamically describe the encoder as a function of a particular input sequence, the number of branches increase as a function of 2^x where x is the number of bits in the input sequence and it becomes practically impossible to continue drawing the tree diagram. It can be observed that the tree diagram repeats after K branches where K is the number of stages of the encoder. Hence the structure can be converted into another diagram called the trellis. The trellis exploits the repetitive structure of the tree and provides a more manageable encoder description. The trellis diagram of the (2,1,2) encoder is given in Fig. 2.4. In this trellis each branch is labelled with two values, input/output and the nodes of the trellis characterise the encoder states.

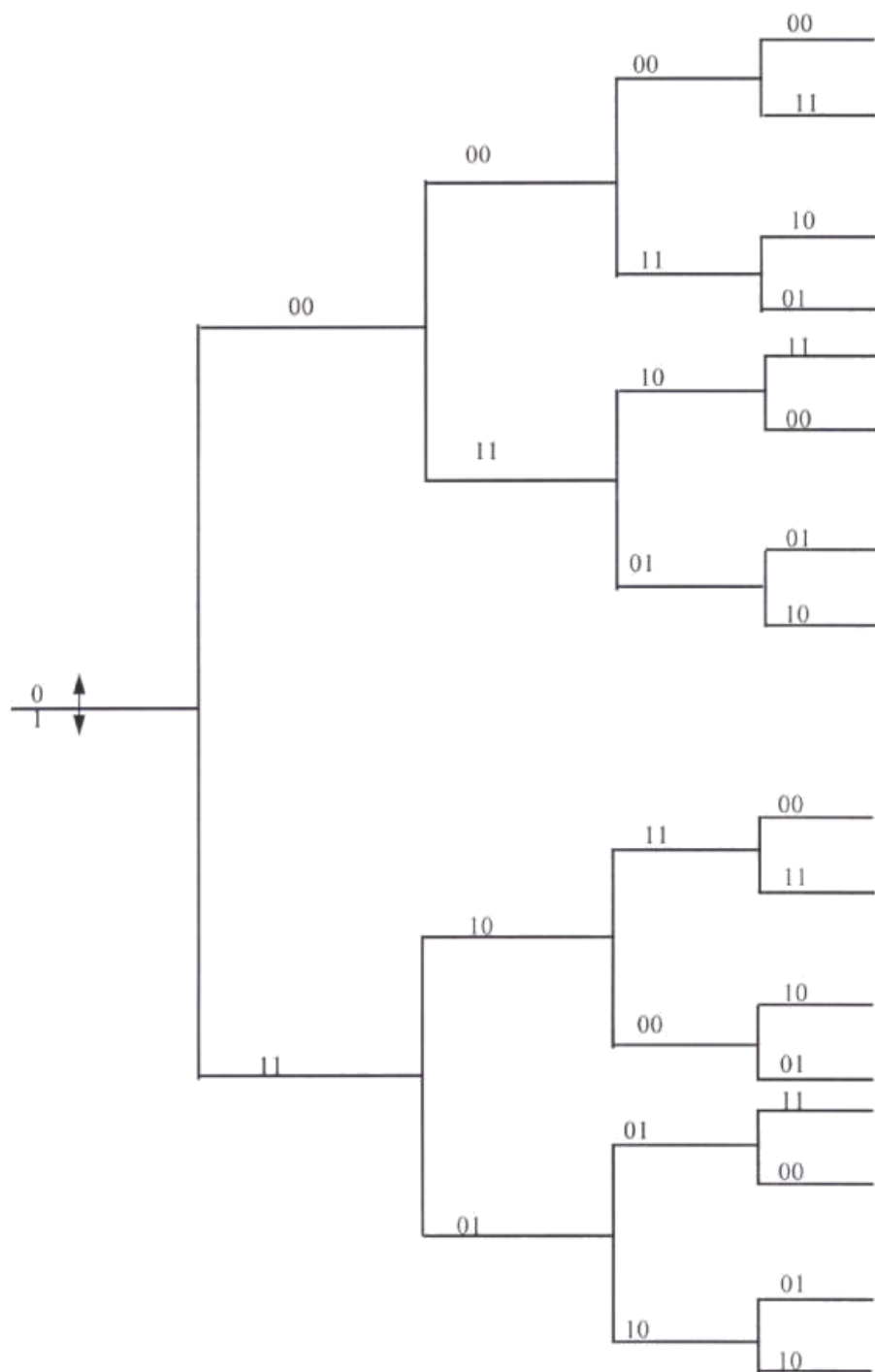


Fig. 2.3. Tree diagram for the (2,1,2) convolutional encoder

2.2.3. The Trellis Diagram

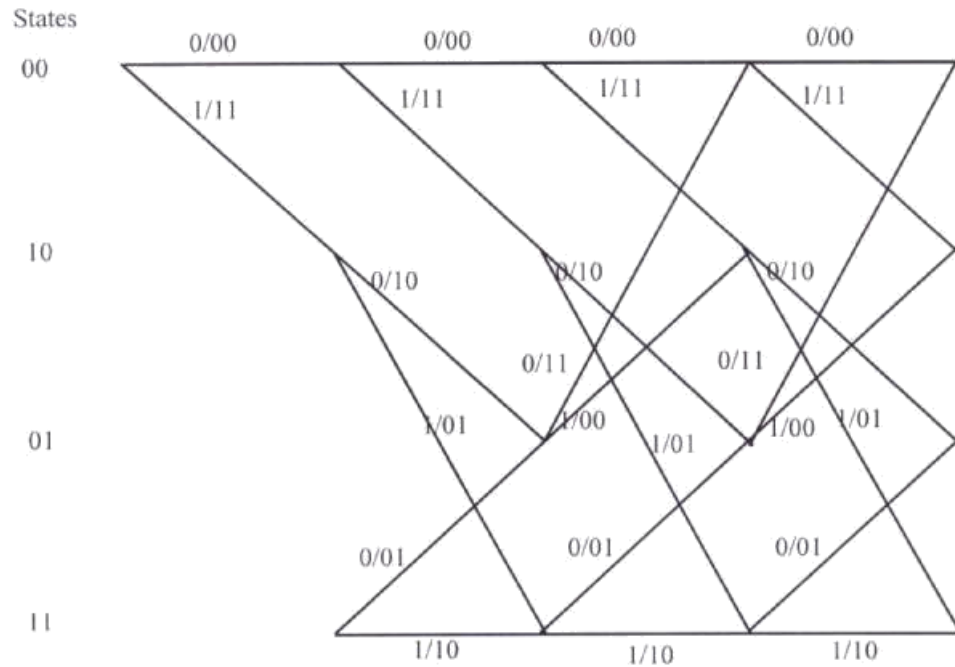


Fig. 2.4. Trellis diagram of the (2,1,2) convolutional encoder

2.3 Block codes

A linear block code is described by two integers n and k , and a generator matrix. The integer k is the number of data bits that forms an input to a block encoder. The integer n is the total number of bits in the associated codeword out of the encoder. A characteristic of linear block codes is that each codeword n -tuple is uniquely determined by the input message k -tuple. The ratio $\frac{k}{n}$ is called the code rate and is a measure of the amount of added redundancy. Therefore in block codes the message sequence is partitioned into blocks, U , of fixed length k , where U is given by

$$U = (u_1, u_2, u_3, \dots, u_k) \quad 2.5$$

The channel encoder maps each input message block U into an n -component output block called the codeword and denoted by

$$V = (v_1, v_2, v_3, \dots, v_n) \quad 2.6$$

where $n > k$.

for binary sequences, there are 2^k possible messages and 2^n possible codewords each referred to as an (n, k) block code. In a linear systematic (n, k) block code of k message bits, the $n-k$ bits are linear combinations of the components of the message bits. Often the two sets are grouped together such that the first $(n-k)$ digits are a linear combination of the components of the message block while the last k digits are the k message digits themselves. Thus

$$v_1 = u_1g_{11} + u_2g_{21} + \dots + u_kg_{k1}$$

$$v_2 = u_1g_{12} + u_2g_{22} + \dots + u_kg_{k2}$$

.

$$v_{n-k} = u_1g_{1n-k} + u_2g_{2n-k} + \dots + u_kg_{kn-k}$$

$$v_{n-k+1} = v_1$$

$$v_{n-k+2} = v_2$$

.

.

$$v_n = v_k \quad 2.7$$

where all additions are modulo-2. Based on the set of equations we can construct a generator matrix given by

$$G = \begin{bmatrix} g_{1,1} & g_{1,2} & \cdot & \cdot & g_{1,n-k} & 1 & 0 & \cdot & \cdot & 0 \\ g_{2,1} & g_{2,2} & \cdot & \cdot & g_{2,n-k} & 0 & 1 & \cdot & \cdot & 0 \\ \cdot & \cdot & \cdot & \cdot & \cdot & \cdot & \cdot & \cdot & \cdot & \cdot \\ \cdot & \cdot & \cdot & \cdot & \cdot & \cdot & \cdot & \cdot & \cdot & \cdot \\ g_{k,1} & g_{k,2} & \cdot & \cdot & g_{k,n-k} & 0 & 0 & \cdot & \cdot & 1 \end{bmatrix}$$

that is $G = [P, I_k]$ where the $k \times (n-k)$ matrix P is the parity matrix and I_k is a $k \times k$ identity matrix. This matrix can equally well be written as $G = [I_k, P]$ since the performance of the code over a memoryless channel is independent of any column permutation in the generator matrix. Thus the components of the codeword V can be produced by considering the k -tuple U as a row vector and performing the multiplication as given in equation 2.1

Every linear block code has another matrix H called its parity check matrix which is given by

$$H = [I_{n-k} P^T] \quad 2.8$$

where I_{n-k} is the $(n-k) \times (n-k)$ identity matrix and P^T is the transpose of the matrix P in G . If we premultiply H^T by V we have

$$VH^T = U[PI_k] \begin{bmatrix} I_{n-k} \\ P \end{bmatrix} = UP + UP = 0 \quad 2.9$$

This implies that any codeword multiplied by H^T is the $n-k$ length zero vector, a property which is useful for error detection and correction. In particular if e is a n -dimensional binary error vector added to V by the channel, then the syndrome s of the received vector defined by the product

$$S = XH^T \quad 2.10$$

becomes

$$S = XH^T = (V + e)H^T = VH^T + eH^T = 0 + eH^T = eH^T \quad 2.11$$

Clearly if X is a codeword then $s = 0$, but if X is not a codeword $S \neq 0$. Thus an error is detected if $S \neq 0$. Also it is useful to note that the syndrome s is independent of the codeword transmitted but depends on the error vector e .

The equation above implies that there are some undetectable error patterns that occur whenever e is not a codeword. Since there are $2^k - 1$ undetectable non zero codewords, there are $2^k - 1$ undetectable error patterns.

The equation $S = eH^T$ gives the $n - k$ equations in n unknown, the components of e . Thus this equation has 2^k solutions, which implies that there are 2^k error patterns for each syndrome. The decoder, however chooses a single error vector out of the 2^k possible error patterns for a given syndrome in such a way that the error pattern chosen minimises the probability of error. For binary symmetric channel, the error vector that minimises the probability of error is the error pattern with the smallest number of 1's. Once e is known, then the transmitted codeword can be calculated using

$$V = X + e \quad 2.12$$

Therefore for each syndrome, the decoder must have available the error vector with the fewest number of 1's out of the corresponding 2^k error patterns. The operation of the channel decoder can be summarised in 3 steps.

Step 1: Calculate the syndrome of the received vector, that is, $s = XH^T$.

Step 2: Find the error vector e with the fewest 1's corresponding to s .

Step 3: Compute the decoder output as $V = X + e$.

An upper bound on the probability of a decoding error (block error) for a t -error correcting block code over a BSC with independent probability of a bit error p is given by

$$P_B \leq \sum_{j=t+1}^n \binom{n}{j} p^j (1-p)^{n-j} \quad 2.13$$

where the right side simply sums up all possible combinations of $t+1$ or more errors.

2.3.1 Array Codes

Array codes were first introduced by Elias [1954] and have been proposed for many burst and random error control applications [Burton and Weldon 1965, Bahl and Chien 1971, Farrell 1979, Farrell and Hopkins 1982, Blaum, Farrell and Van Tilborg 1986, Blaum and Farrell 1988, Honary and Kaya 1991 and others]. Array codes are constructed from component codes assembled in two and more dimensions and have a simple structure and low complexity implementation [Honary et al. 1993a]. The aim behind such construction being:

- (i) the construction of more powerful code structures from simple subcodes.
- (ii) the low decoding complexity of the resulting code.

2.3.2 Single Parity Check Code

The Single Parity Check (SPC) code is obtained by adding a single parity digit (even parity) to a block of k information digits, that is, if the information digits are $X_1, X_2, X_3, \dots, X_k$ then the parity digit P_{k+1} is given by

$$P_{k+1} = X_1 \oplus X_2 \oplus X_3 \oplus \dots \oplus X_{k-1} \oplus X_k \quad 2.14$$

where \oplus denotes modulo-2 addition. A single parity check code can be described as an (n, k) code where $n = k+1$. The single parity check code has a generator matrix given by

$$G = \begin{bmatrix} g_1 \\ g_2 \\ . \\ . \\ g_k \end{bmatrix} = \begin{bmatrix} 1 & 0 & 0 & . & . & 0 & 1 \\ 0 & 1 & 0 & . & . & 0 & 1 \\ . & . & . & . & . & . & . \\ . & . & . & . & . & . & . \\ 0 & 0 & 0 & . & . & 1 & 1 \end{bmatrix}$$

Therefore if $X = [x_1 \ x_2 \ x_3 \ . \ . \ . \ x_k]$ is the information vector, then the single parity check code has a minimum Hamming distance of 2. Hence it can detect any odd number of errors in a code and it can correct single erasures.

2.3.3 Row and Column (RAC) Array Codes

The row and column array codes [Farrell 1979] is the simplest form of two-dimensional array codes. The two array codes are also referred to as rectangular codes [Patel and Hong 1974], two co-ordinate codes [Rowland 1968] and matrix codes [Voukalis 1980]. These codes may be square or rectangular in shape. The information

digits are put into an array of k_1 rows and k_2 columns. The single parity check operation is performed on rows and columns to obtain an array with n_1 rows and n_2 columns, the code is represented as $(n_1, k_1, 2)(n_2, k_2, 2)$ or $(n, k, 4)$ where $n = n_1 n_2$ and $k = k_1 k_2$. The code rate is given by

$$R = \frac{k}{n} = \frac{k_1 k_2}{n_1 n_2} = \frac{(n_1 - 1)(n_2 - 1)}{n_1 n_2} \quad 2.15$$

For a given block length the code rate is maximised for square codes. The structure of a RAC array code is given in Fig.2.5

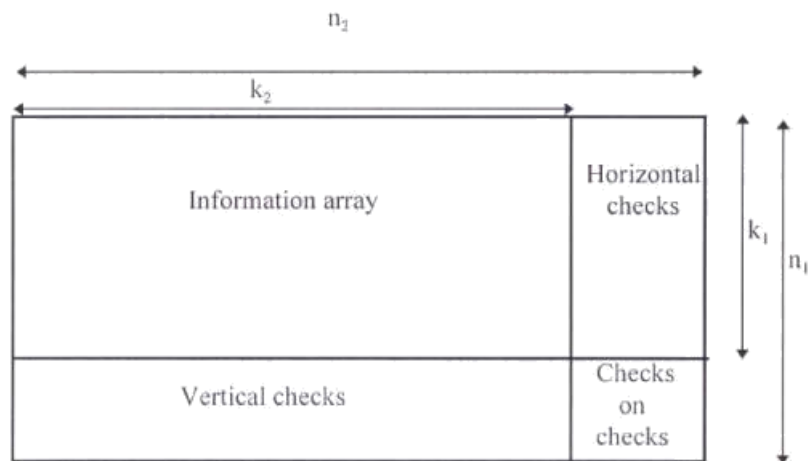


Fig. 2.5 Structure of an RAC array code

An example of an RAC array code is

$$\begin{bmatrix} x_{11} & x_{12} & \cdot & \cdot & \cdot & x_{1k_2} & p_{1n_2} \\ x_{21} & x_{22} & \cdot & \cdot & \cdot & x_{2k_2} & p_{2n_2} \\ \cdot & & & & & \cdot & \cdot \\ \cdot & & & & & \cdot & \cdot \\ \cdot & & & & & \cdot & \cdot \\ x_{k_11} & \cdot & \cdot & \cdot & \cdot & x_{k_1k_2} & p_{k_1n_2} \\ p_{n_11} & \cdot & \cdot & \cdot & \cdot & p_{n_1k_2} & p_{n_1n_2} \end{bmatrix}$$

where $x_{ij}(i=1,2,3\dots k_1, j=1,2,3,\dots,k_2)$ represent the information bits and $p_{in_2}(i=1,2,3,\dots,n_1)$ and $p_{n_1j}(j=1,2,3,\dots,n_2)$ represents the rows and columns parity check bits respectively. The generator matrix of a RAC array code is obtained from the kronecker product of the single parity check code generator matrices [Slepian 1960]. This kronecker product is also known as a tensor product [Wolf 1965]. The generator matrix of a row SPC code with k_1 information bits is given by

$$G^r = \begin{bmatrix} g_1^r \\ g_2^r \\ \cdot \\ \cdot \\ g_{k_1}^r \end{bmatrix} = \begin{bmatrix} 1 & 0 & \cdot & \cdot & \cdot & 0 & 1 \\ 0 & 1 & \cdot & \cdot & \cdot & 0 & 1 \\ \cdot & \cdot & & & & \cdot & \cdot \\ \cdot & \cdot & & & & \cdot & \cdot \\ 0 & 0 & \cdot & \cdot & \cdot & 1 & 1 \end{bmatrix}$$

Similarly the generator matrix of a column SPC with k_2 information digits is given by

$$G^r = \begin{bmatrix} g_1^c \\ g_2^c \\ \cdot \\ \cdot \\ g_{k_2}^c \end{bmatrix} = \begin{bmatrix} 1 & 0 & \cdot & \cdot & \cdot & 0 & 0 \\ 0 & 1 & \cdot & \cdot & \cdot & 0 & 0 \\ \cdot & \cdot & & & & \cdot & \cdot \\ \cdot & \cdot & & & & \cdot & \cdot \\ 1 & 1 & \cdot & \cdot & \cdot & 1 & 1 \end{bmatrix}$$

The generator matrix of the RAC code G is obtained from the product of G^r and G^c .

The G matrix has $k_1 k_2$ rows and $n_1 n_2$ columns and is given by [Kaya 1993c]

$$G = \begin{bmatrix} g_1 \\ \vdots \\ g_{k_1} \\ g_{k_1+1} \\ \vdots \\ g_i \\ g_{i+1} \\ \vdots \\ g_{k_1 k_2} \end{bmatrix} = \begin{bmatrix} g_{11}^r g_1^c & g_{12}^r g_1^c & \cdot & \cdot & \cdot & \cdot & g_{1n_1}^r g_1^c \\ \vdots & \vdots & & & & & \vdots \\ \vdots & \vdots & & & & & \vdots \\ g_{11}^r g_{k_1}^c & g_{12}^r g_{k_1}^c & \cdot & \cdot & \cdot & \cdot & g_{1n_1}^r g_{k_1}^c \\ g_{21}^r g_1^c & g_{22}^r g_1^c & \cdot & \cdot & \cdot & \cdot & g_{2n_1}^r g_1^c \\ \vdots & \vdots & & & & & \vdots \\ \vdots & \vdots & & & & & \vdots \\ g_{21}^r g_{k_1}^c & g_{22}^r g_{k_1}^c & \cdot & \cdot & \cdot & \cdot & g_{2n_1}^r g_{k_1}^c \\ g_{k_1 1}^r g_1^c & g_{k_1 2}^r g_1^c & \cdot & \cdot & \cdot & \cdot & g_{k_1 n_1}^r g_1^c \\ \vdots & \vdots & & & & & \vdots \\ \vdots & \vdots & & & & & \vdots \\ \vdots & \vdots & & & & & \vdots \\ g_{k_1 1}^r g_{k_1}^c & g_{k_1 2}^r g_{k_1}^c & \cdot & \cdot & \cdot & \cdot & g_{k_1 n_1}^r g_{k_1}^c \end{bmatrix}$$

The codeword can be obtained as the product

$$V = X \cdot G \quad 2.16$$

If we take the (3,2) row code and the (3,2) column code that have generator matrices given by

$$G^r = \begin{bmatrix} g_1^r \\ g_2^r \end{bmatrix} = \begin{bmatrix} 1 & 0 & 1 \\ 0 & 1 & 1 \end{bmatrix};$$

$$G^c = \begin{bmatrix} g_1^c \\ g_2^c \end{bmatrix} = \begin{bmatrix} 1 & 0 & 1 \\ 0 & 1 & 1 \end{bmatrix};$$

Then

$$G = \begin{bmatrix} 1 & 0 & 0 & 0 & 0 & 0 & 1 & 0 & 0 \\ 0 & 1 & 1 & 0 & 0 & 0 & 0 & 1 & 1 \\ 0 & 0 & 0 & 1 & 0 & 1 & 1 & 0 & 1 \\ 0 & 0 & 0 & 0 & 1 & 1 & 0 & 1 & 1 \end{bmatrix}$$

and the encoded codeword \mathbf{V} for an information bit sequence $\mathbf{U} = 0001$ is given by \mathbf{V} where $\mathbf{V} = \mathbf{UG} = 000011011$

The weight distribution of the RAC array code are $w_0=1$, $w_4=9$, $w_6=6$, where w_i represents a weight of i

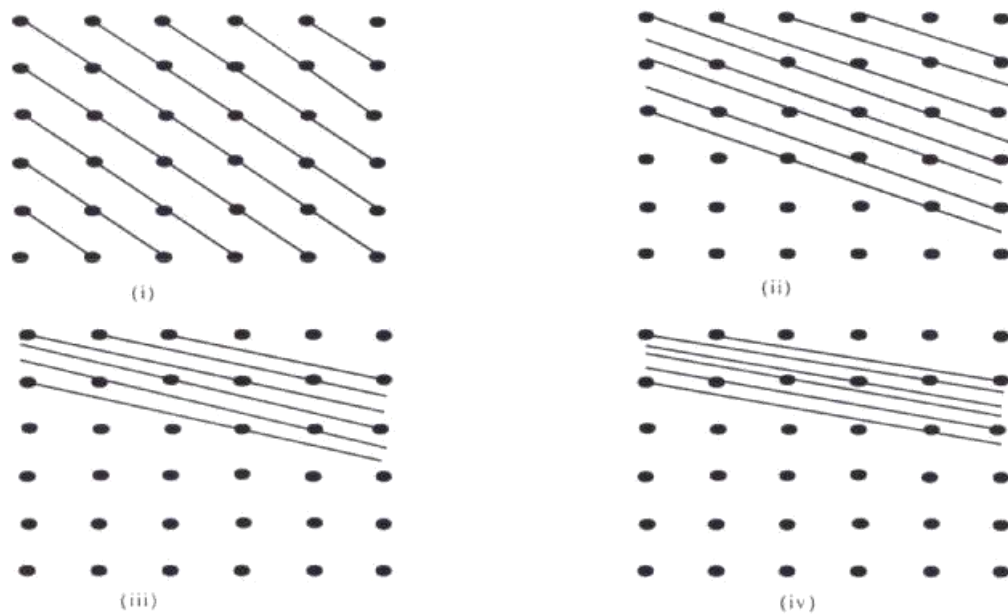


Fig. 2.6 Diagonal checks on an information array; (i) 1-1 diagonal checks (ii) 1-2 diagonal checks (iii) 1-3 diagonal checks (iv) 1-4 diagonal checks

2.3.4 Diagonals Checks Array Codes

The error control power of the array code can be increased by performing parity check diagonally in addition to the row and column parity checks. Voukalis[Voukalis 1980]

and Daniel [Daniel 1985] have investigated codes with these structures and some possible diagonal checks are given in Fig. 2.6.

2.3.5 Folded Diagonal Checks Array Codes

Simple use of RAC parity check is not a very efficient way to increase the error control capability of a code, since the redundancy increases faster than the error correcting power obtained from the redundant bits. In order to improve the power of the code the parity check bits need to be made more efficient by folding them round the information array as shown below:

$$\begin{bmatrix} 1 & 2 & 3 & 4 \\ 5 & 6 & 7 & 8 \\ 9 & 10 & 11 & 12 \\ 1 \oplus 5 \oplus 9 & 2 \oplus 6 \oplus 10 & 3 \oplus 7 \oplus 11 & 4 \oplus 8 \oplus 12 \\ 4 \oplus 7 \oplus 10 & 1 \oplus 8 \oplus 11 & 5 \oplus 2 \oplus 12 & 9 \oplus 6 \oplus 3 \end{bmatrix}$$

The column parities together with the folded diagonal parity checks results in a (20,12,4) array code. Alternately the folded checks can be combined with the column parity checks as

$$\begin{bmatrix} 1 & 2 & 3 & 4 \\ 5 & 6 & 7 & 8 \\ 9 & 10 & 11 & 12 \\ 1 \oplus 5 \oplus 9 \oplus 4 \oplus 7 \oplus 10 & 2 \oplus 6 \oplus 10 \oplus 1 \oplus 8 \oplus 11 & 3 \oplus 7 \oplus 11 \oplus 5 \oplus 2 \oplus 12 & 4 \oplus 8 \oplus 12 \oplus 9 \oplus 6 \oplus 3 \end{bmatrix}$$

This gives the (16,12,3) array code. The combination of the folded parity checks with the column checks improves the code rate

2.3.6 Multidimensional Array Codes

Certain efficient codes are obtained by taking parity checks on the information array formed in three or more dimensions. The subcodes used to make the multidimensional array can be single parity check codes or more powerful codes. The parameters of an M-dimensional array code are

$$(n,k) = (n_1 n_2 n_3 \dots n_m, k_1 k_2 k_3 \dots k_m) \quad 2.17$$

and the minimum Hamming distance d_{\min} is given by $d_{\min} = d_1 d_2 d_3 \dots d_m$, where the components subcodes are (n_1, k_1, d_1) , (n_2, k_2, d_2) , and (n_m, k_m, d_m) .

2.4 Generalised Array Codes

Array codes, such as product codes and concatenated codes are constructed by combining other codes [Elias 1954]. Simple RAC array codes may be square or rectangular and have the parameters $(n,k,d_{\min}=4)$, where n is the number of bits in the code, k is the number of information bits and d_{\min} is the code's Hamming distance. These codes although flexible to design and simple to decode have a lower value of k than other linear block codes of the same size and Hamming distance. Honary et al. [Honary et al. 1993b] have proposed another block array code called generalised array code (GAC) which is based on the augmentation of the RAC array code by superimposing repetition codes on parity row and/or columns.

2.4.1 GAC Code Construction

A generalised (n,k,d_{\min}) array code is an array code in which the columns and rows subcodes may have different numbers of information and parity check symbols; the code length $n = n_1 n_2$ and the total length of the information digits

$$k = k_1 + k_2 + k_3 + \dots + k_{n_2} \quad 2.18$$

where n_1 and n_2 represent the number of rows and columns respectively and k_p is the number of information digits in the p th row. The procedures for designing a linear generalised array code (n_0, k_0, d_0) [Honary et al. 1995a] which can also be described as an array representation of coset codes introduced by Forney [Forney 1988] are:

(i) design a binary array code $C_1 (n, k, d_{\min})$ as shown in Fig. 2.7a., with single parity check rows and columns and $R_1 = (n_2, k_2, d_2)$ row codes, where $d_2 = \left\lfloor \frac{d_0}{2} \right\rfloor$ where $\lfloor x \rfloor$ denotes the nearest greatest integer. If n_0 is a prime number we choose $n = n_0 + 1$.

(ii) design a binary $n_1 n_2$ product code $C_2 = |PA|$, as shown in Fig. 2.7b. where P is a binary $k_2 n_1$, array with only parity check elements; A is a binary $(n_2 - k_2) n_1$, matrix where the first row consists of only $k' = n_2 - k_2$ information digits and all columns are repetition codes.

(iii) If there is information digits left over design a third binary product code C_3 as in Fig. 2.7c., Where $B = (n_1, 1, d_0)$ is a repetition row code with k_0 th information digit.

(iv) add the designed coded as follows:

$$C = C_1 \oplus C_2 \oplus C_3 \quad 2.19$$

where \oplus is a modulo-2 addition.

(v) if $n = n_0 + 1$, delete the symbol which is located in the n_1 th row and n_2 th column

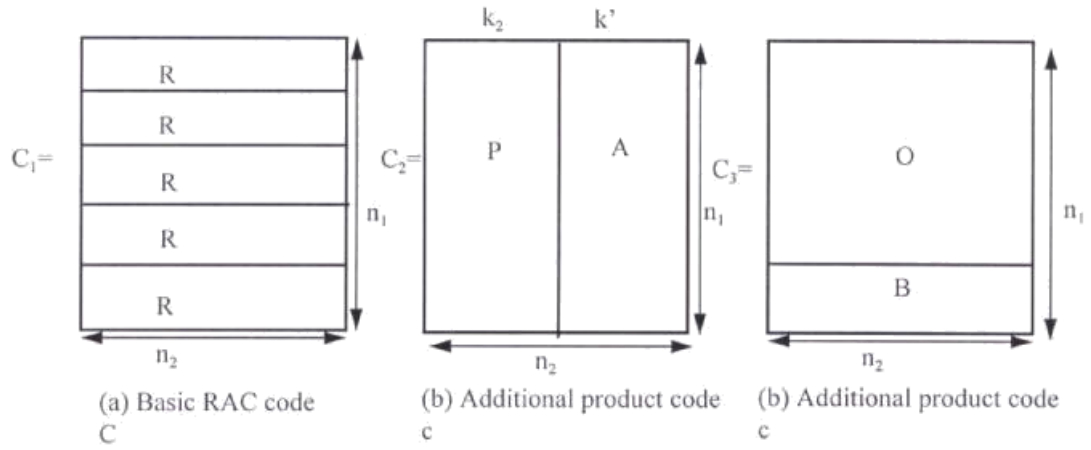


Fig. 2.7. Code Structure

2.4.2 Design of (8,4, 4) and (7,4,3) Codes

The (8,4,4) GAC is equivalent to the RM code [Lin and Costello 1983, Peterson and Weldon 1975]. The procedures for the design of this code are:

- (i) Design the basic (8,3,4) array code C_1 with single parity checks (4,3,2) columns and (2,1,2) repetition row codes.

$$C_1 = \begin{bmatrix} x_1 & p_1 \\ x_2 & p_2 \\ x_3 & p_3 \\ p_4 & p_4 \end{bmatrix}$$

- (ii) Design an additional array code $C_2 = |PA|$ with the structure

$$C_2 = \begin{bmatrix} 0 & x_4 \\ 0 & x_4 \\ 0 & x_4 \\ 0 & x_4 \end{bmatrix}$$

where x_4 is an information digit and P is an all zero column.

(iii) since all information digits have been used, there is no additional array code C_3 .

(iv) Add the two codes C_1 and C_2 using modulo-2 addition to obtain C as

$$C = C_1 \oplus C_2 = \begin{bmatrix} x_1 & x_4 \oplus p_1 \\ x_2 & x_4 \oplus p_2 \\ x_3 & x_4 \oplus p_3 \\ p_4 & x_4 \oplus p_4 \end{bmatrix}$$

(v) Since $n_0 = n$, there is no need to delete the parity check symbol on row 4 and column 2. This is a non systematic code and has a weight distribution of $w_0 = 1$, $w_4=14$ and $w_8 = 1$., where w_i is a weight of i . This weight distribution is similar to that of the (8,4,4) RM code. Deleting the symbol at row 4 and column 2 gives the (7,4,3) Hamming code:

$$C = \begin{bmatrix} x_1 & x_4 \oplus p_1 \\ x_2 & x_4 \oplus p_2 \\ x_3 & x_4 \oplus p_3 \\ p_4 \end{bmatrix}$$

2.4.3 Design of (15,7,5) Code

(i) Design the basic (15,4,6) product code C_1 :

$$C_1 = \begin{bmatrix} x_1 & x_2 & p_1 & p_2 & p_3 \\ x_3 & x_4 & p_4 & p_5 & p_6 \\ p_7 & p_8 & p_9 & p_{10} & p_{11} \end{bmatrix}$$

where x_i $i=1,2,...,4$ represents information digits and p_j $j=4,5,...,11$ represents parity check symbols.

(ii) Design two additional product codes C_2 and C_3 with the structures

$$C_2 = \begin{bmatrix} 0 & 0 & p_{12} & x_5 & x_6 \\ 0 & 0 & p_{12} & x_5 & x_6 \\ 0 & 0 & p_{12} & x_5 & x_6 \end{bmatrix}$$

$$C_3 = \begin{bmatrix} 0 & 0 & 0 & 0 & 0 \\ 0 & 0 & 0 & 0 & 0 \\ x_7 & x_7 & x_7 & x_7 & x_7 \end{bmatrix}$$

where x_i $i=5,6,7$ are information bits and $p_{12} = x_5 \oplus x_6$.

(iii) Add C_1 , C_2 and C_3 using modulo 2 to obtain C :

$$C = C_1 \oplus C_2 \oplus C_3 = \begin{bmatrix} x_1 & x_2 & p_1 \oplus p_{12} & x_3 \oplus p_2 & x_6 \oplus p_2 \\ x_3 & x_4 & p_4 \oplus p_{12} & x_5 \oplus p_5 & x_6 \oplus p_5 \\ p_7 \oplus x_7 & p_8 \oplus x_8 & x_7 \oplus p_9 \oplus p_{12} & x_5 \oplus x_7 \oplus p_{10} & x_6 \oplus x_7 \oplus p_{11} \end{bmatrix}$$

the designed code has the following parameters: $(n_0=15, k_0=7, d_0=5)$

2.5 Trellis design technique for RAC codes

The trellis design procedure is as follows:

(1) The number of states, N_s , in the trellis is given by

$$N_s = q^{k_2} \quad 2.20$$

(2) The trellis depth (number of columns in the trellis) N_c is then given by

$$N_c = k_1 + 2$$

2.21

(3) Identify each state at depth p (where p can take all values between 0 and N_c-1 inclusive) by a k_2 tuple q -ary vector

$$S^p(A) = S^p(a_1, a_2, a_3, \dots, a_j, \dots, a_{k_2}) \quad 2.22$$

where a_j is an element of $GF(q)$, and $j = 1, 2, \dots, k_2$.

(4) Mark the trellis diagram starting at depth $p=0$ and finishing at $p=N_c-1$ with

$S^0(0_1, 0_2, \dots, 0_{k_2})$ and $S^{k_1+1}(0_1, 0_2, \dots, 0_{k_2})$ states respectively.

(5) The trellis branches at each depth p are labelled by a k_1 -tuple q -ary vector C_A^p ,

where C_A^p is determined using

$$C_A^p(B) = S^p(A) \oplus S^{p+1}(A) \quad 2.23$$

where A and B are all possible k_2 -tuple q -ary vectors that represent the present (p) and the next ($p+1$) states of the trellis respectively, and \oplus is mod q addition.

(6) Each branch is labelled by two particular values:

$$C_A^p(a_1, a_2, \dots, a_{k_2})$$

which represents the input information symbols and

$$D_A^p(a_1, a_2, \dots, a_{k_2+1})$$

which represents the output vector where

$$a_{k_2+1} = \sum_{i=1}^{k_2} a_i$$

and Σ denotes modulo 2 addition.

This algorithm gives the correct trellis for all codes square or rectangular. Consider, for example, the $(3,2,2)(4,3,2)$ array code. Using the above algorithm we obtain the following:

$$(1) N_s = 2^{k_2} = 2^3 = 8$$

$$(2) N_c = k_1 + 2 = 2 + 2 = 4$$

This gives a trellis depth of four that matches the three rows of information exactly.

Also equation given in step 5 is obeyed since A and B are vectors of the same order.

The trellis structure of the $(3,2,2)(4,3,2)$ array code is illustrated in Fig. 2.8.

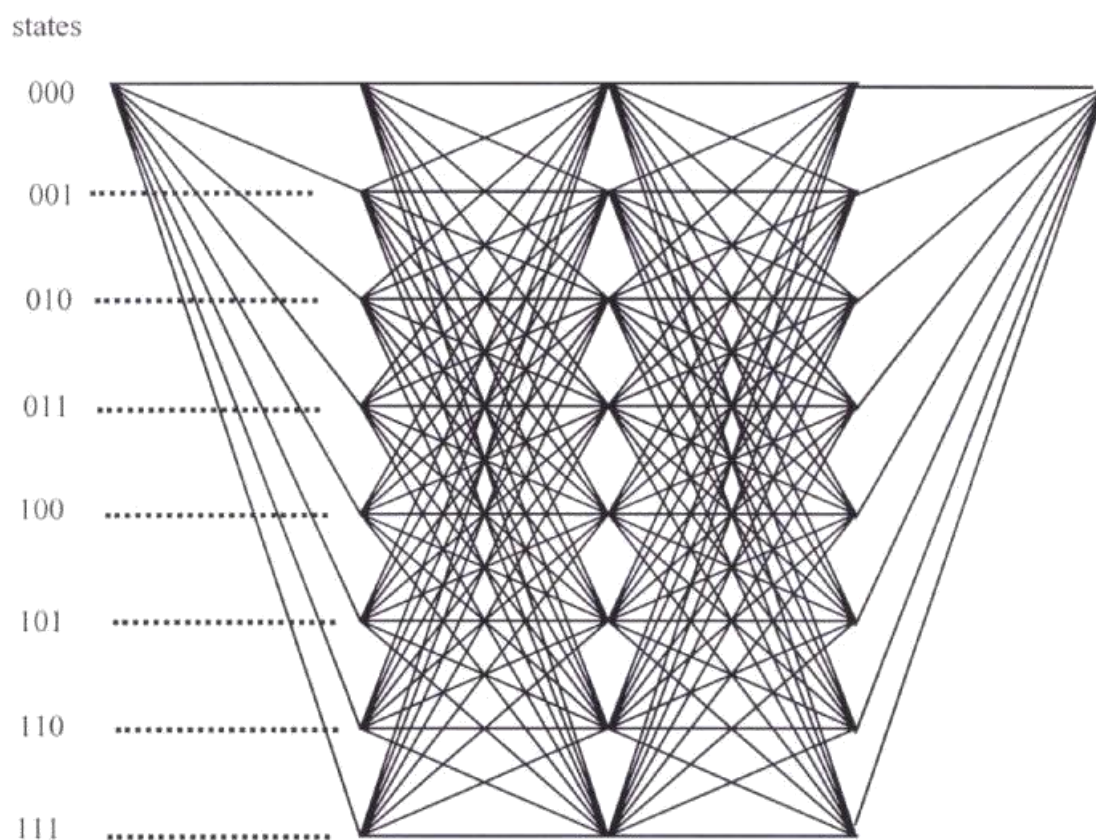


Fig. 2.8 Trellis structure of the $(3,2,2)(4,3,2)$ RAC array code

2.6 Low Complexity Trellis Decoding of Linear Block Codes

Trellis decoding of linear block codes has been under investigation since 1974 [Bahl, Cocke, Jelinek and Raviv 1974, Wolf 1978, Massey 1978] Later, a number of soft decision maximum likelihood decoding algorithms for block codes were proposed [Conway and Sloane 1986, Kasami et al. 1993, Be'ery and Synders 1986]. Forney [Forney 1988, Forney and Trott 1993] and others [Kasami et al. 1993, Muder 1988, Berger and Be'ery 1993] have stimulated interest in low complexity trellis decoding of block codes for both practical and theoretical reasons. Recently Honary et al. [Honary, Markarian, and Darnell 1995a] have proposed low complexity trellis design of a wide range of block codes. This trellis design procedure is described in the next section in this chapter.

2.6.1 Trellis Design Procedure of Linear Block Codes

The trellis design procedure for linear block codes is an extension of the trellis design procedure of Generalised Array Codes (GAC). A linear block code like a Generalised Array Code can be represented as a set of row subcodes $(n_2, k_1, d_1), (n_2, k_2, d_2), \dots, (n_2, k_{n_1}, d_{n_1})$ where n_2 is the number of columns in the code and k_1, k_2, \dots, k_{n_1} are the number of information bits in rows 1, 2, 3, ..., n_1 . For each such code the generator matrices are G_1, G_2, \dots, G_{n_2} respectively.

The trellis design procedure [Honary et al. 1993a, Honary et al. 1995a] is as follows:

(I) Choose the trellis depth N_c and the number of states N_s as

$$N_c = n_1 + 1 \quad 2.24$$

$$N_s = 2^{\max k_p} \quad 2.25$$

(ii) Identify each state at depth p by a $\{k_p\}$ -tuple binary vector $S_p(A)$ where $S_p(A)$ is given by

$$S_p(A) = S_p(a_1, a_2, \dots, a_j, \dots, a_{\max\{k_p\}}) \text{ where } a_j = 0, 1$$

(iii) The trellis branches start at depth $p=0$ and ends at depth $p=n_2$; these are labelled as $S_0(00\dots 0)$ and $S_{n_2}(00\dots 0)$ respectively.

(iv) The trellis branches at depth p are labelled X_p/C_p where X_p represents the k_p -tuple binary vectors of information digits for the p th row and C_p corresponds to the encoded codewords in the p th row and is obtained from:

$$C_p = X_p^1 G_p + C_p^2 \quad 2.26$$

where G_p is the generator matrix for the p th row code and X_p^1 and C_p^2 are codewords from the p th rows of the C_1 and C_2 codes respectively.

(v) There are 2^{k_p} branches starting from each state $S_p(A)$ at depth $p, (<N_c)$ each branch is connected with state $S_{p+1}(A)$ at depth $p+1$, which is defined as follows:

$$S_{p+1}(A_j) = S_p(A_i) + X_p \quad 2.27$$

(vi) If a second additional code, C_3 , is used for a code design, at the final depth all states must be connected to the final state $S_n(00\dots 0)$ with two parallel branches; the labels of these branches complement to each other.

There are

$$N_0 = \prod_{p=1}^{n_2} 2^{k_p} \quad 2.28$$

distinct paths through this trellis diagram and each path corresponds to a unique codeword from the code.

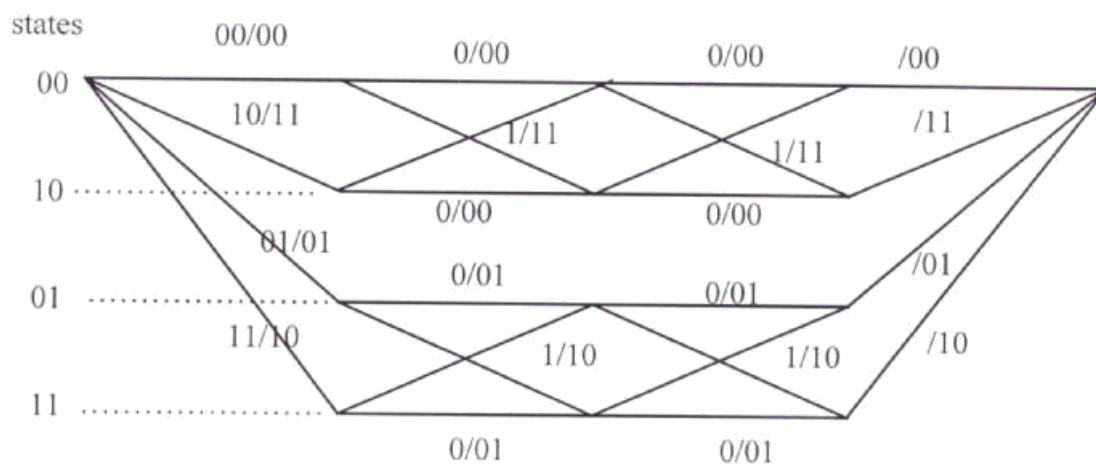


Fig. 2.9 Trellis structure of the (8,4,4) GAC code

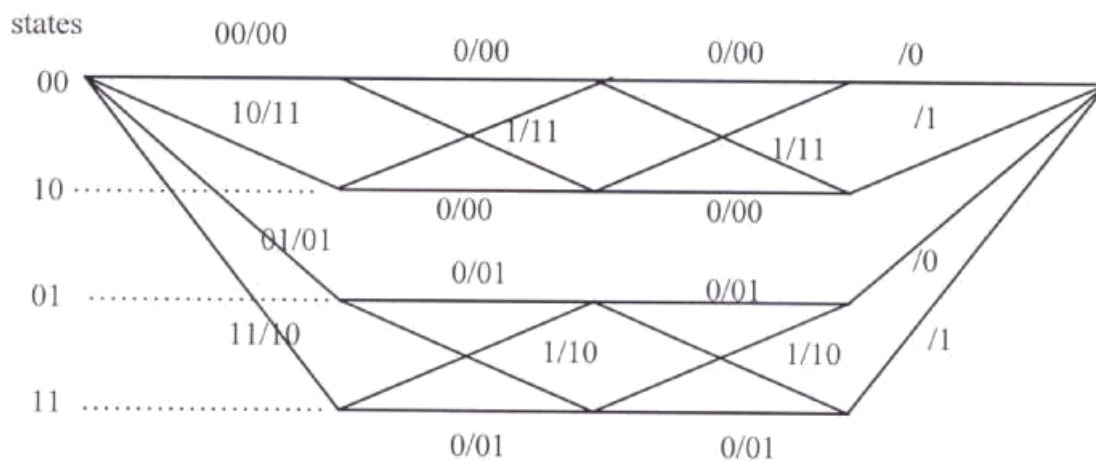


Fig. 2.10 Trellis structure of the (7,4,3) Hamming code

2.6.2 Trellis Diagrams of the (8,4,4) GAC and (7,4,3) Hamming codes

Following the technique outlined above, the trellis diagram of the (8,4,4) code will have $N_c = 4 + 1 = 5$, and $N_s = 2^2 = 4$

We identify the states by a 2-tuple binary vectors and at depth $p=0$ and $p=5$ the trellis has only one state, namely $S_0(00)$ and $S_4(00)$, respectively. The trellis diagram of the $(8,4,4)$ GAC code is given in Fig 2.9. The trellis diagram of the $(7,4,3)$ Hamming code Fig. 2.10 is similar to the trellis of the $(8,4,4)$ and differs only in the number of digits being used for labelling the branches at the final depth.

3.7.3 Trellis structure of the $(9,6,3)$ GAC code

Following the same procedures we obtain the trellis structure of the $(9,6,3)$ GAC code shown in Fig. 2.11.

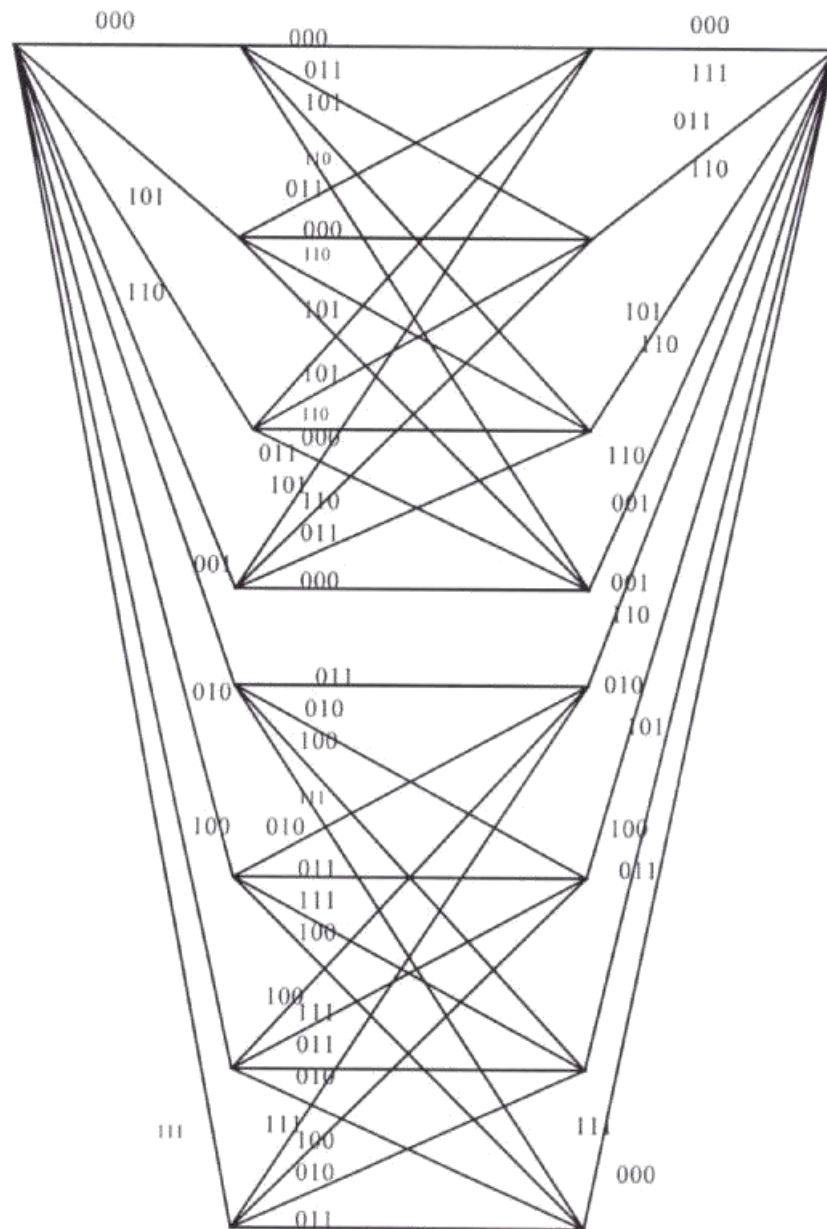


Fig 2.11 Trellis diagram of the (9,6,3) GAC code

Chapter 3

Embedded Coding Technique using Linear Block Codes

3.1 Introduction

Embedded coding technique [Darnell 1983, Darnell et al.1988, Darnell et al 1989, Zolghadr et al. 1988] employs a combination of forward error correction and detection(FEC/FED) for error control in and ARQ environment. In this scheme, a concatenated code [Forney 1976] with an inner code for error correction and an outer code for error detection is used. Block formatted data are transmitted at several different rates simultaneously in an Automatic Repeat Request (ARQ) type communication [Darnell 1983, Lin and Costello 1983, Lin, Costello and Miller 1984, Yu and Lin 1981]. After each block the receiver indicates to the transmitter the highest rate at which it has been able to detect the data in the previous interval. The retransmission strategy determines the system throughput; three basic methods exists [Lin and Costello 1983,Lin, Costello and Miller 1984]. These are

- (i) stop and wait
- (ii) go-back-N
- (iii) selective repeat

The assumption behind the embedded coding technique is that at least one of the rates will normally be received successfully over a wide range of channel conditions. It has been shown [Darnell et al. 1988, Darnell et al 1989, Zolghadr et al. 1988] that the embedded scheme yields high reliability over a wide range of input bit error rates.

The code comprises two main codes A_1 and A_2 , where A_1 is called the inner code and A_2 is called the outer code. A_1 is a combination of three inner codes C_1 , C_2 , and C_3 respectively capable of correcting F_1 , F_2 and F_3 or fewer errors such that $F_1 > F_2 > F_3$ and

$$F_i = \left\lfloor \frac{d_i - 1}{2} \right\rfloor$$

where i is an integer given by $i = 1, 2, 3$, d_i is the code C_i Hamming distance, and $\lfloor x \rfloor$ denotes the integer part of x . This scheme can be regarded as a hybrid ARQ scheme [Farrell, Honary, Bate, 1988] in which the information packets are encoded in the same block, using codes of decreasing error correcting capability. Thus at time when the error probability is relatively high, only the sub-block encoded with the most powerful code may be accepted, at the expense of low overall code rate and a subsequent reduction in the system's throughput efficiency [Lin and Costello 1983]. However when the signal to noise ratio is high, even the sub-blocks encoded with the least powerful code are also accepted, resulting in an increase in the system's throughput efficiency.

This kind of technique has applications in situations where the transmission capacity of the communication varies with time, such as the HF medium ranging from 3 to 30 MHz. This has been shown by many authors to be one of the most severe channels for the transmission of binary data [Brayer and Cardinale 1967, Juresek et al. 1971], on which channel error rates of 0.001 to 0.01 are quite common. Apart from its use in very bad channels, embedded coding technique has other applications such as in fixed capacity channels, for example, in the transmission of vocoded digitised speech, in

which the significance of the digits describing the pitch is considerably greater than those specifying other parameters of the speech encoding model [Jewett and Cole 1978, Goodman and Sunberg 1984]. In such circumstances it is possible to encode the more significant digits of the data stream using the inner code. This minimises the overall distortion.

3.2 Embedded Code Encoding/Decoding Procedures

In order to encode a message of k information digits and to decode the received codeword, Darnell et al. [Darnell et al. 1988] have proposed the following procedures:

- (i). The message of k information bits is divided into four information sub-blocks

$$\{k_1, k_2, k_3, k_4\}$$

- (ii). Each sub-block is then encoded in a manner depending on its position in the main block, using the inner codes as shown in Fig. 3.1.

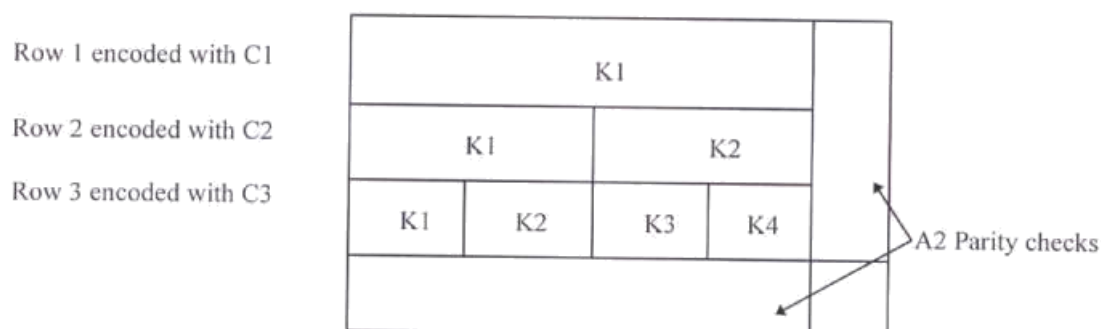


Fig. 3.1 Structure of an embedded code

- (iii). The outer code A_2 is then applied to the inner codes information blocks to produce an encoded block for transmission.

In the decoding process, the inner decoders perform error correction within each of the sub-block codes followed by error detection by the outer decoder. Therefore, a received block is first acted on by the inner decoders and depending on the number of errors present within each sub-block, these may or may not be successfully corrected. The corrected sub-blocks are stored in the outer decoder's buffer. The outer decoder then performs error detection in the sub-blocks stored in the buffer starting from the first and proceeding to the fourth. It accepts the errorfree sub-blocks and requests for a retransmission of the other sub-blocks. Darnell et al. [Darnell et al. 1988] have compared the (52,12) embedded array code with a conventional (52,36) array code using hard decision decoding. They have shown that the embedded encoding method yields a high reliability at very high bit error rates (e.g. 0.1) and that although the throughput efficiency of the embedded technique is greatly reduced due to added redundancy of the inner codes, for high channel bit error rates (e.g. 0.05-0.1), the embedded system results in an improved throughput efficiency. Also the array code would cease to operate effectively at a channel BER greater than 0.001, while the embedded code would continue to perform successively under these conditions [Zolghadr 1989].

3.2.1 Modified Embedded Array Code

Darnell et al. [Darnell et al. 1988] have further shown that the (52,12) embedded array code suffers from low throughput in regions of low to moderate channel BER. This is the direct result of the additional redundancy of the repeated sub-blocks in the main body of the encoded block. Since in the region of low channel BER the uncoded information packets are accepted with the greatest probability, it is unnecessary to

transmit the encoded information packets. They have subsequently proposed a modified version of the embedded code shown in Fig. 3.2, where each information packet consists of one information digit.

K1 K1 K1 K1 K1					K2 K2 K2 K2				K3 K3 K3 K3 K3					P1	
K4 K4 K4			K5 K5			K6 K6 K6			K7 K7 K7			K8 K8 K8			P2
K9	K10	K11	K12	K13	K14	K15	K16	K17	K18	K19	K20	K21	K22	K23	P3
P19	P18	P17	P16	P15	P14	P13	P12	P11	P10	P9	P8	P7	P6	P5	P4

Fig. 3.2 (64,23) modified embedded array code block structure

The encoding/decoding procedure and the protocols used for this code are the same as the embedded encoding method. The decoding of these array codes was still hard decision decoding and not maximum-likelihood using trellis structure.

3.2.2 Embedded Convolutional Code

Zolghadr et al. [Zolghadr et al. 1988] have proposed a scheme of embedded convolutional code based on the puncturing of the code to obtain different rates convolutional codes. The embedded convolutional code is shown in Fig. 3.3. It consists of three streams each encoded independently using convolutional codes of rates $1/2$, $2/3$, and $3/4$. Each encoded stream consists of 12 bits and so the number of information bits in each stream is 6, 8, and 9 respectively.

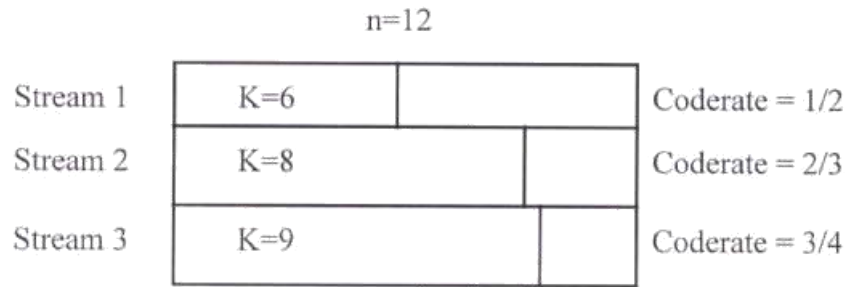


Fig. 3.3 Embedded Convolutional code block

In order to encode the data they used a $\frac{1}{2}$ rate convolutional encoder the output of which they partitioned into sub-blocks of length 12, 16, and 18 bits. Then depending on the desired rate of a given sub-block, a number of bits were deleted from each sub-block according to a deleting map. The resulting sub-blocks were then transmitted over the channel. The deleting map is also known at the receiver, which is kept in bit synchronisation with the transmitter, thus allowing the receiver to insert erasures for the deleted bits. Their results showed that the embedded convolutional code replaced the original repetition codes in the embedded code (that was responsible for the low throughput efficiency) and so increased the throughput efficiency of the embedded convolutional code. Further, these results showed that the embedded convolutional code performs well in environment where the channel SNR varies continuously, that is, both the throughput and reliability of the system are improved compared with the fixed rate FEC convolutional code.

In this chapter three embedded codes based on linear block codes and trellis decoding [Honary et al 1993a, Honary et al 1993b, Honary et al 1993c Honary et al 1995] are proposed.

3.3 Embedded Code employing Linear Block Code and Trellis

Decoding

The embedded array code described is based on the embedded block encoding procedure of Darnell et al. [Darnell, Honary and Zolghadr 1988] as shown in Fig. 3.4.

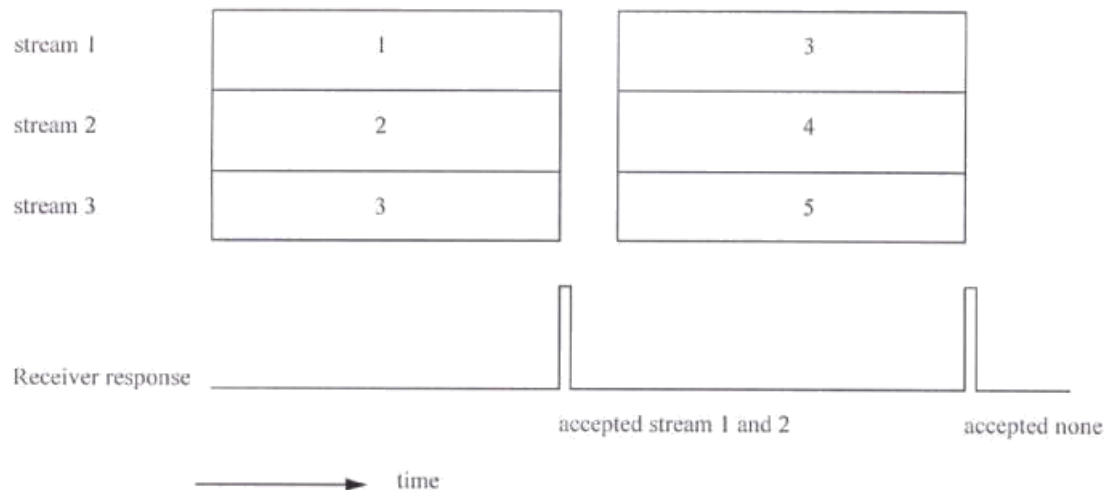


Fig. 3.4 ARQ protocol of the embedded code

The embedded array code employs proposed RAC and GAC codes, whilst retaining the desirable reliability performance of the embedded code. The embedded code comprises two main codes, D_1 and D_2 . D_1 consists of three codes each having the same dimensions and D_2 is the outer parity check code.

3.3.1 The Overall System

The overall system shown in Fig. 3.5 comprises the following elements:

- (i) data source generating binary data
- (ii) encoder consisting of three array encoders
- (iii) transmitter buffer
- (iv) transmitter, channel and receiver
- (v) 11 level quantiser
- (vi) trellis decoders
- (vii) error limiter
- (viii) feedback channel
- (ix) output buffer and sink.

The transmitter and receiver operate at baseband using bipolar signalling. The transmitted levels are set at +1 and -1 volts, corresponding to binary digits 1 and 0 respectively. The channel is assumed to be slow Rayleigh faded and affected by AWGN with a mean of zero and a standard deviation of σ . The quantiser first limits the input analogue voltage (signal plus noise) to the range -1V to +1V. This voltage interval is then sampled into 11 levels. The resulting samples therefore vary from 0.0 to 1.0 in steps of 0.1.

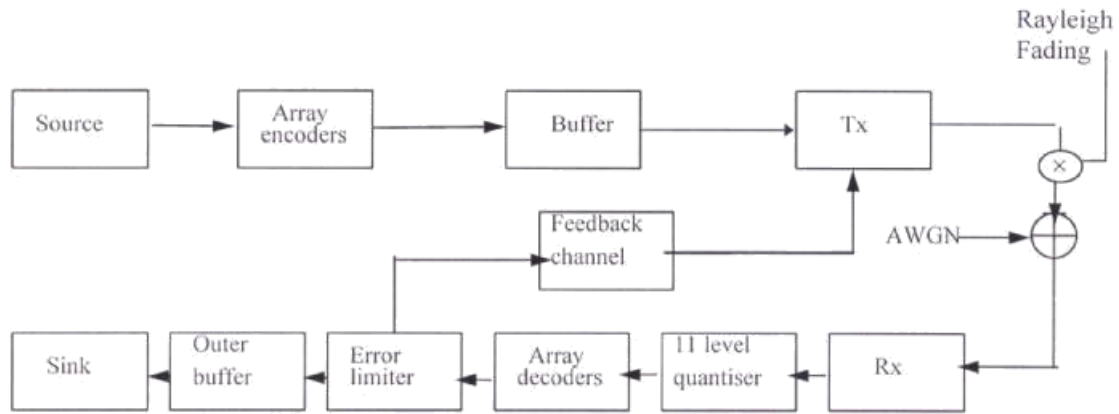


Fig. 3.5 System block diagram

3.3.2 Embedded Code Encoding Procedures

The main block comprises two codes D_1 and D_2 . D_1 consists of three streams, each encoded independently using the codes C_1 , C_2 , and C_3 that are respectively the (16,5,8) GAC, (16,9,4) RAC and the (16,11,4) GAC. The coderates are $\frac{5}{16}$, $\frac{9}{16}$ and $\frac{11}{16}$ and they possess decreasing error correcting capability. The structure of the embedded code is shown in Fig. 3.6.

The encoding is performed as follows:

- (i) A message of 25 bits is divided into three information sub-blocks {5,9,11}
- (ii) Each sub-block is then encoded in a manner described previously depending on its position in the main block using the array codes C_1 , C_2 , and C_3 where C_1 , C_2 , and C_3 are as shown below:
- (iii) The outer code D_2 is then applied to the inner codes blocks to produce an encoded block for transmission.

These resulting sub-blocks are then transmitted.

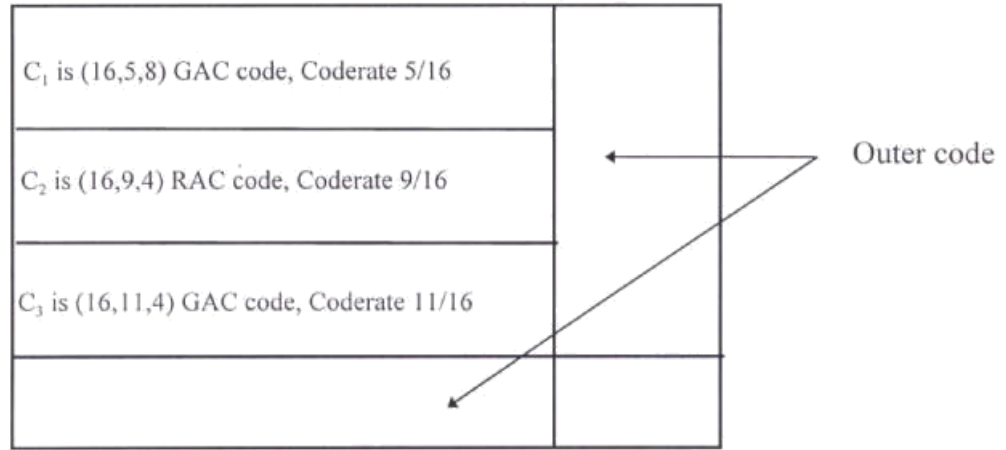


Fig. 3.6 Structure of Embedded code employing linear block codes

$$C_1 = \begin{bmatrix} x_1 & p_1 & p_1 & p_1 \\ x_2 & p_2 & p_2 & p_2 \\ x_3 & p_3 & p_3 & p_3 \\ p_4 & p_4 & p_4 & p_4 \end{bmatrix} \oplus \begin{bmatrix} 0 & x_4 & x_5 & x_4 \oplus x_5 \\ 0 & x_4 & x_5 & x_4 \oplus x_5 \\ 0 & x_4 & x_5 & x_4 \oplus x_5 \\ 0 & x_4 & x_5 & x_4 \oplus x_5 \end{bmatrix}$$

$$= \begin{bmatrix} x_1 & p_1 \oplus x_4 & p_1 \oplus x_5 & p_1 \oplus x_4 \oplus x_5 \\ x_2 & p_2 \oplus x_4 & p_2 \oplus x_5 & p_2 \oplus x_4 \oplus x_5 \\ x_3 & p_3 \oplus x_4 & p_3 \oplus x_5 & p_3 \oplus x_4 \oplus x_5 \\ p_4 & p_4 \oplus x_4 & p_4 \oplus x_5 & p_4 \oplus x_4 \oplus x_5 \end{bmatrix}$$

$$C_2 = \begin{bmatrix} x_6 & x_7 & x_8 & p_5 \\ x_9 & x_{10} & x_{11} & p_6 \\ x_{12} & x_{13} & x_{14} & p_7 \\ p_{11} & p_{10} & p_9 & p_8 \end{bmatrix}$$

$$\begin{aligned}
C_3 &= \begin{bmatrix} x_{15} & x_{16} & x_{17} & p_{12} \\ x_{18} & x_{19} & x_{20} & p_{13} \\ x_{21} & x_{22} & x_{23} & p_{14} \\ p_{18} & p_{17} & p_{16} & p_{15} \end{bmatrix} \oplus \begin{bmatrix} 0 & 0 & 0 & x_{24} \\ 0 & 0 & 0 & x_{24} \\ 0 & 0 & 0 & x_{24} \\ x_{25} & x_{25} & x_{25} & x_{24} \oplus x_{25} \end{bmatrix} \\
&= \begin{bmatrix} x_{15} & x_{16} & x_{17} & p_{12} \oplus x_{24} \\ x_{18} & x_{19} & x_{20} & p_{13} \oplus x_{24} \\ x_{21} & x_{22} & x_{23} & p_{14} \oplus x_{24} \\ p_{18} \oplus x_{25} & p_{17} \oplus x_{25} & p_{16} \oplus x_{25} & p_{15} \oplus x_{24} \oplus x_{25} \end{bmatrix}
\end{aligned}$$

3.3.3 The Decoder

The decoder performs two main tasks: (i) soft decision maximum likelihood trellis decoding of the linear block codes in order to correct the errors and (ii) error detection. The inner decoders perform error correction within each of the sub-block codes followed by error detection by the outer decoder. The error detector limits the output error probability of the overall system. The error correction within the sub-blocks C_1 , C_2 , and C_3 is realised by using the trellis decoders of Figs. 3.7, 3.8, and 3.9. The corrected sub-blocks are stored in the outer decoder's buffer. The outer decoder then performs error detection in the sub-blocks stored in the buffer. It accepts the error free sub-blocks and requests for a retransmission of the other sub-blocks.

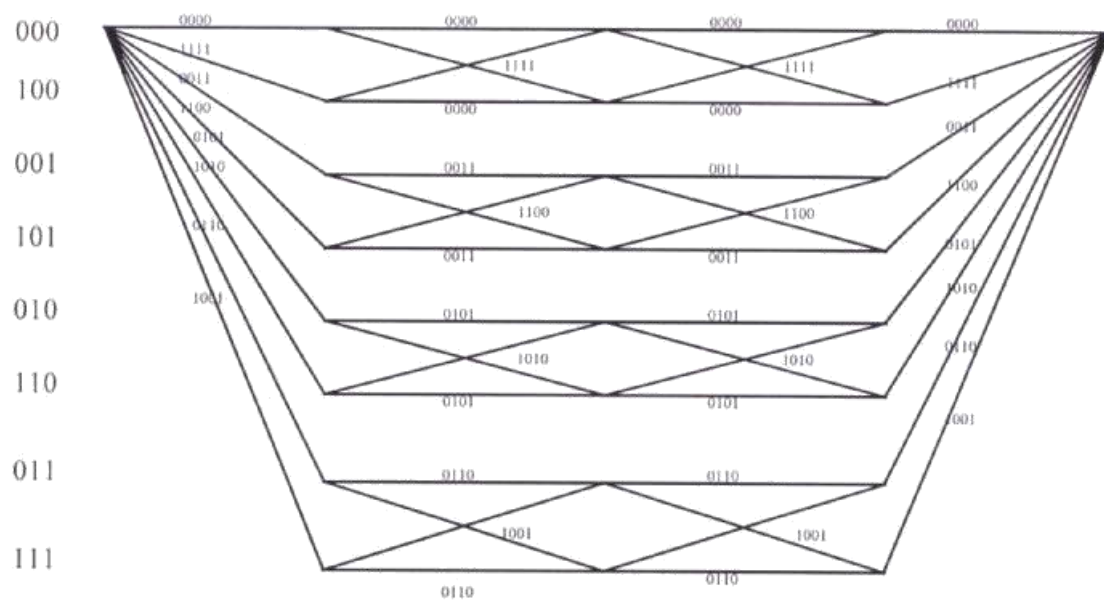


Fig. 3.7 Trellis diagram of the (16,5,8) GAC code

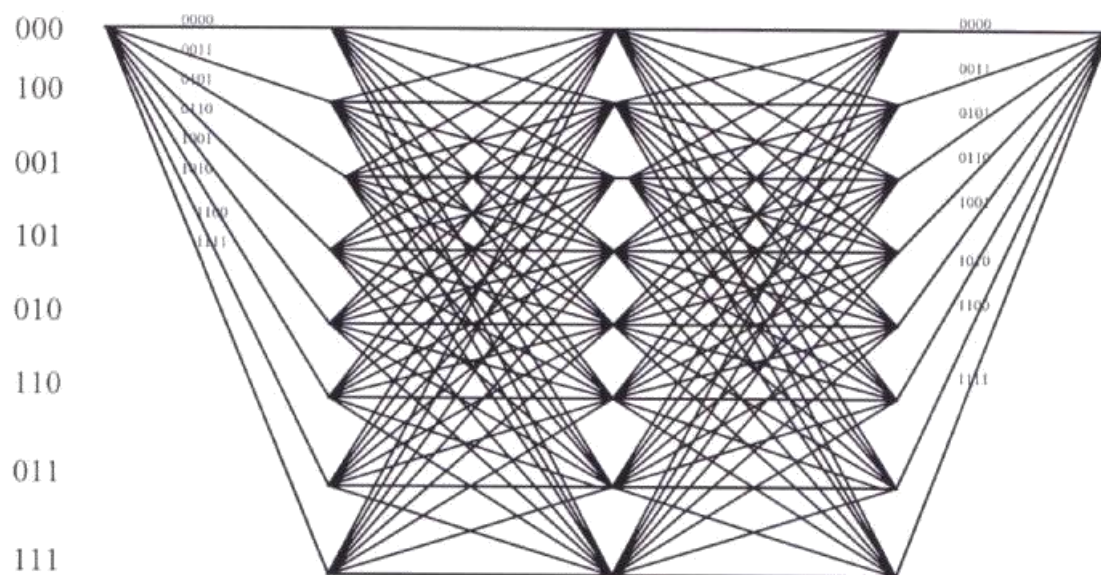


Fig. 3.8 Trellis diagram of the (16,9,4) RAC

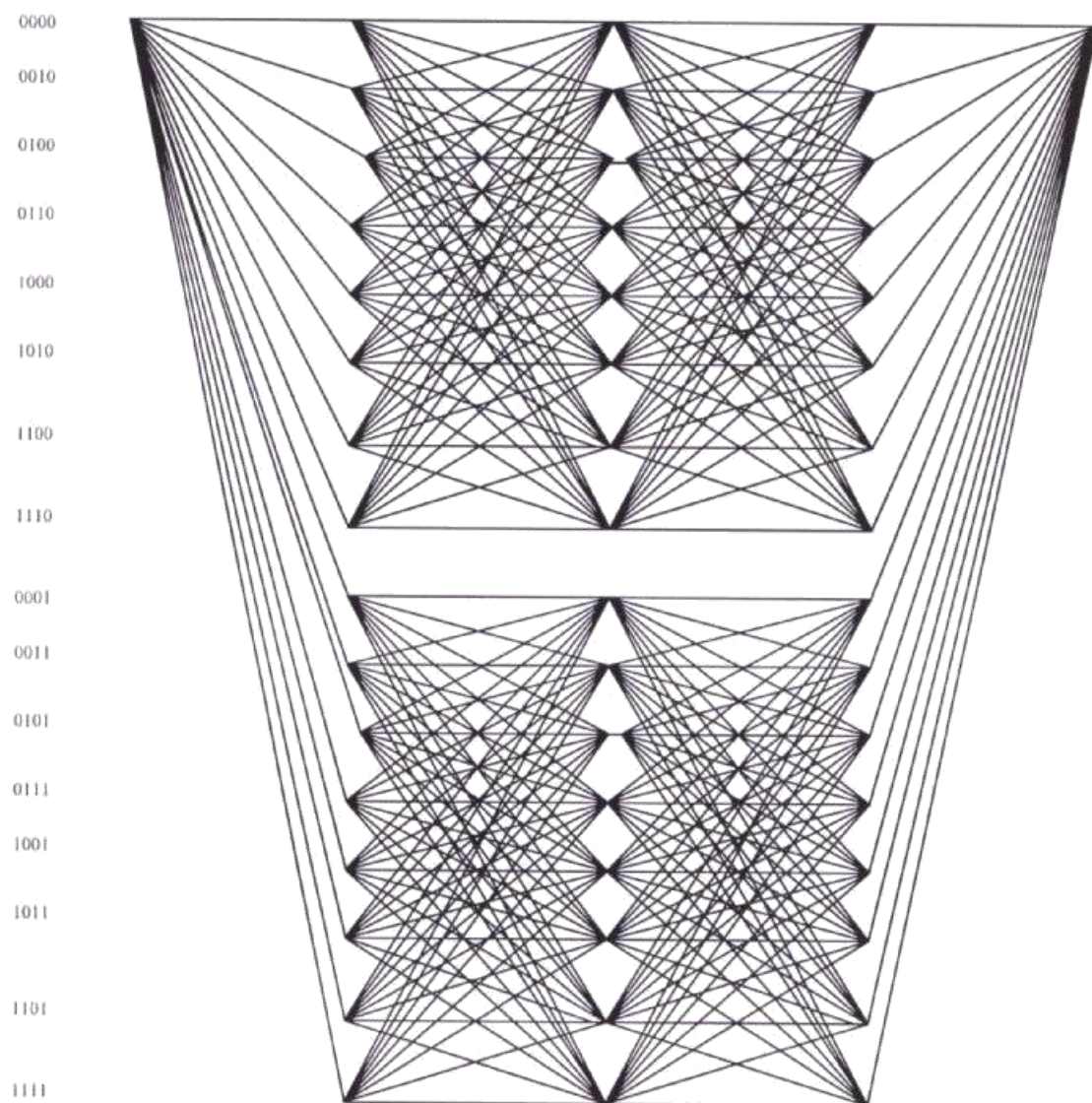


Fig. 3.9 Trellis structure of the (16,11,4) GAC code

3.4 Simulation Results and Discussions

The simulation tests were carried out under Rayleigh fading and AWGN channel conditions. The results presented here are for BPSK signalling scheme. For all cases perfect bit and block synchronisation are assumed. Fig 3.10 shows the effect of the channel SNR on the BER of the three array codes. Suppose we wish to use the embedded codes for transmission when the error rate exceeds 10^{-3} . It can be seen from Fig.3.10 that none of the codes C_1 , C_2 , and C_3 will be accepted until the SNR exceeds about 6.0 dB. C_1 is accepted beyond about 6.0 dB while C_2 and C_3 are respectively accepted beyond about 12 and 14 dB respectively. Figs. 3.11 and 3.12 respectively give the reliability and the throughput efficiency of the codes. Comparison of the embedded code and the (65,48,4) RAC array code shows that the embedded code yields a high reliability at very high bit error rates (for example at a BER of 0.01). Although the throughput efficiency of the embedded technique is greatly reduced due to the redundancy of the code C_1 for low channel BER (below 0.075), the embedded system gives an improved throughput for channel BER above 0.075. It is therefore clear that if the transmission rate of the array codes is reduced so that the errorfree throughputs of the two codes are the same, the reliability of the RAC array code would be superior to that of the embedded code. However the RAC array code would cease to operate effectively at a channel BER greater than 0.075 while the embedded code would continue to perform successfully under these conditions. The disadvantage of the embedded code considered above is that the outer code adds additional redundancy and so reduces the system's throughput. An alternative scheme of embedded code is proposed in the next section. This new scheme does not employ

an outer code and hence has less redundancy. The error detection and error limiting function is performed by the trellises of the components codes.

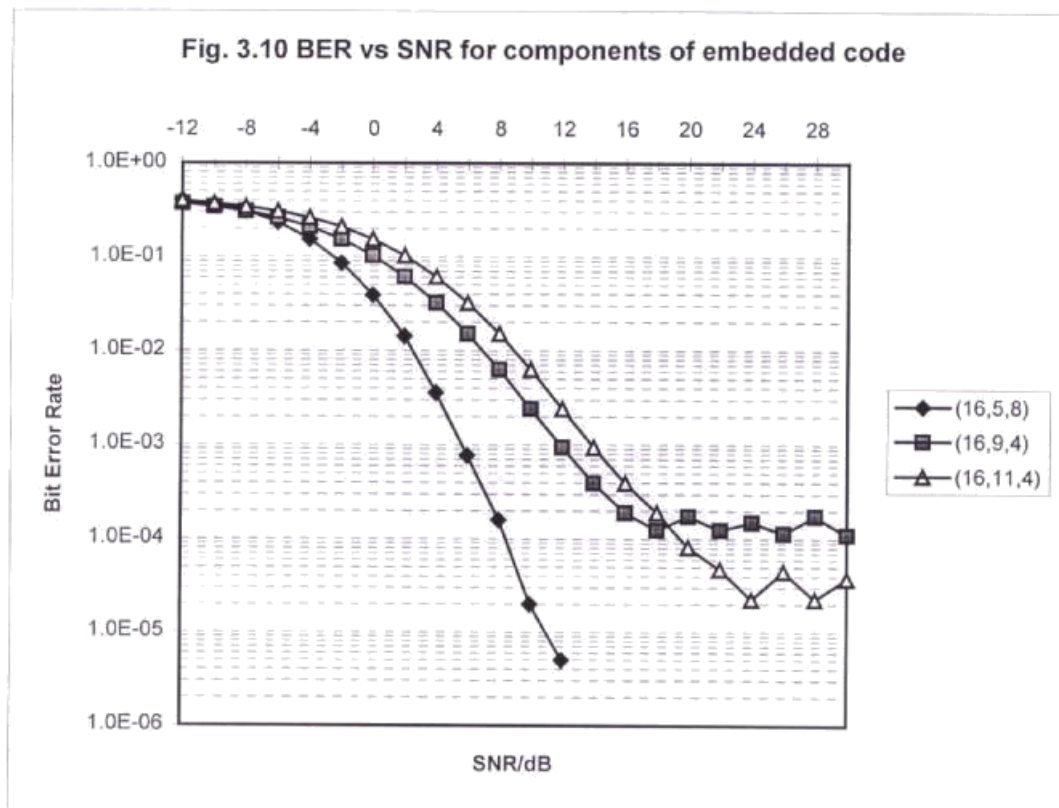


Fig. 3.11 Output BER vs Channel BER for embedded and (65,48,4) RAC code

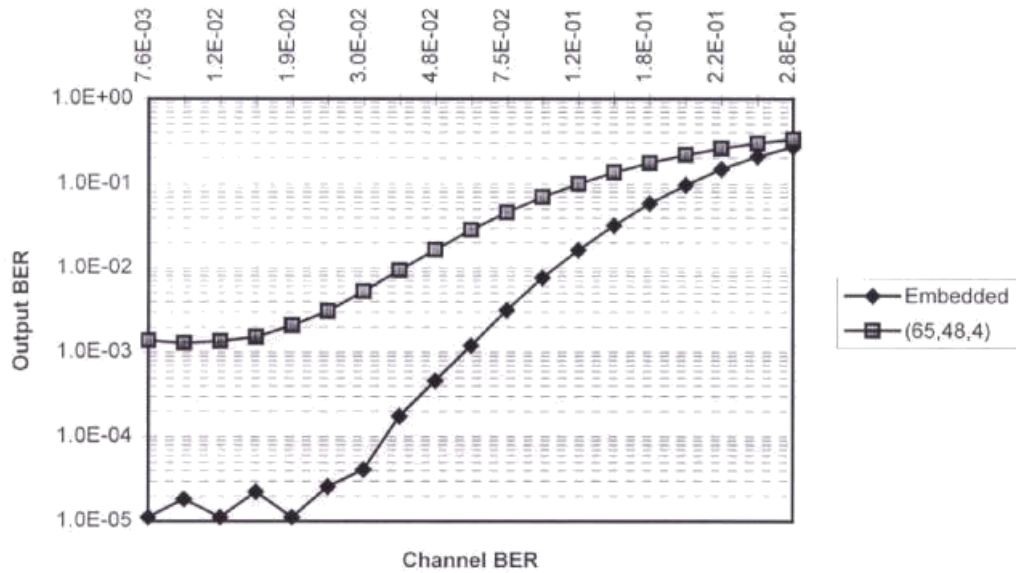
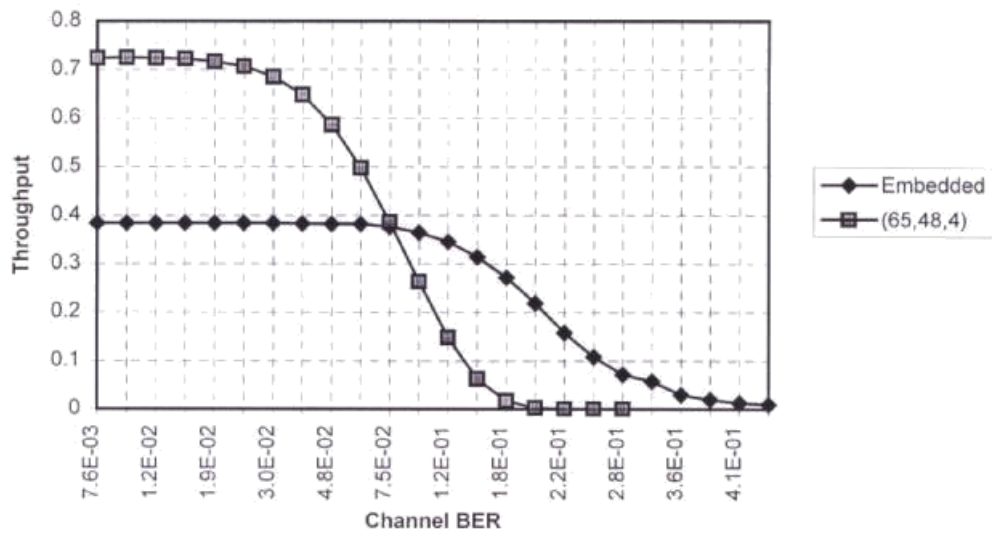
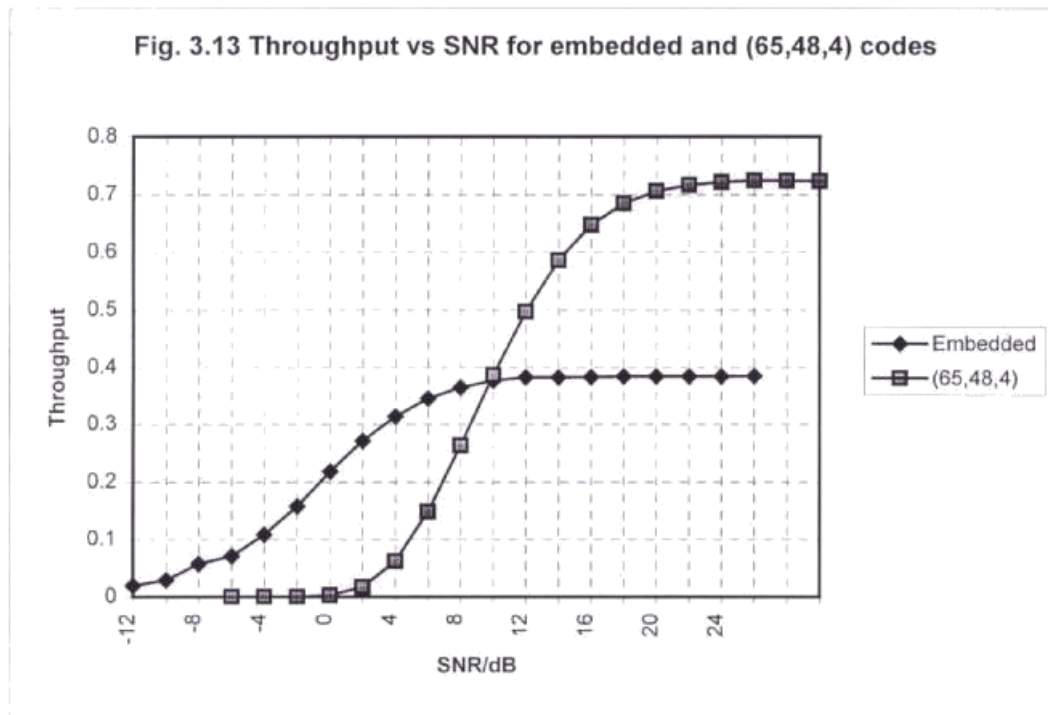


Fig. 3.12 Throughput vs Channel BER for embedded and (65,48,4) codes





3.5 Modified Embedded Code employing Linear Block Codes

The main block consists of three streams, each encoded independently employing the codes C_1 , C_2 , and C_3 that are respectively the (16,5,8) GAC, the (16,9,4) RAC and the (16,11,4) GAC codes used in the original embedded code proposed. The structure of the code is given in Fig. 3.14.

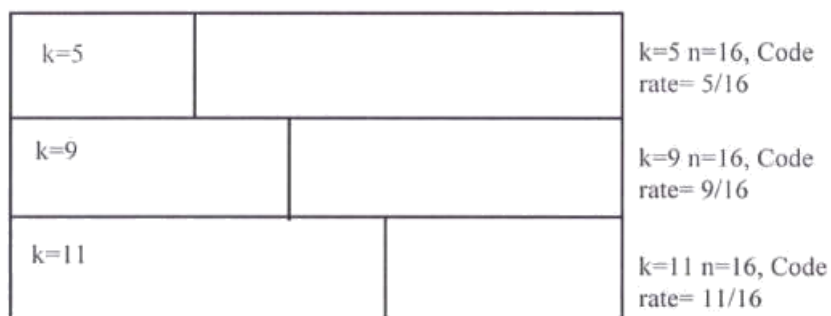


Fig. 3.14 Structure of the modified embedded code employing linear block codes

The encoding is performed as follows:

- (i) A message of 25 bits is divided into three information sub-blocks {5,9,11}
- (ii) Each sub-block is then encoded in a manner described previously depending on its position in the main block using the array codes C_1 , C_2 , and C_3 .

The resulting sub-blocks are then transmitted.

3.5.1 The Decoder

The decoder comprises two main elements, soft decision maximum likelihood trellis decoders for the decoding of the array codes and an error limiter. The error limiter limits the output error probability of the overall system. This is done by considering the Euclidean distance between the correct path chosen by the decoder and the most likely error path. This difference is termed the error detection metric. The error limiter subsequently initiate an ARQ signal for the decoded stream whose error detection metric falls below a given threshold. This scheme is a form of adaptive hybrid ARQ in which information bits are encoded in the same block using codes of decreasing error correcting capability. Thus when the channel is relatively errorfree all the streams are accepted giving a high throughput efficiency, but under noisy conditions only the streams encoded with the most powerful code is accepted leading to a reduction in the throughput efficiency.

The decoder performs two main functions, namely

- (1)Error correction within each sub-block
- (2)Evaluation of error detection metric for the output decoded data.

The error correction within the sub-blocks C_1 , C_2 , and C_3 is realised by using the trellis decoders of Figs. 3.7., 3.8.,and 3.9.

3.5.2 Statistical Channel Evaluation employing the Trellis of the Linear Block Codes

Statistical channel evaluation employing the trellises of GAC codes is explained next. Statistical channel evaluation employing the trellises of RAC array is conducted in a similar manner. In soft decision maximum likelihood decoding of GAC codes, the received voltage levels are divided into a number of levels, say 11 levels. All voltages less or equal to -1 is converted to 0.0 and voltages greater or equal to 1.0 are converted into 1.0. The voltage interval between -1.0 and 1.0 volts are equally divided and grouped in levels in steps of 0.1, such that there are 11 levels in all. The Euclidean distances between the branch values and the quantised received data are determined for each branch in the trellis. This gives us N_s Euclidean distances, that is, one at each node, at depth $p=1$. The Euclidean distance from a node at depth 1 is separately added to the Euclidean distance between a branch value and the received quantised signals for each branch emanating from that node. At depth 2, 3, 4, ..., N_c-2 , there are $p < N_s$ cumulative Euclidean distances at each node, where p is the number of branches terminating at each node. We select the minimum Euclidean distance at each node and proceed to the next depth in the same way. Hence there are only N_s Euclidean left at the final depth N_c-1 . At this node we select the minimum Euclidean distance in order to trace out the maximum likelihood path. The next higher Euclidean distance corresponds to the maximum likelihood error path. The maximum likelihood error path differs from the maximum likelihood path in at least two branches. The difference in the Euclidean distance between these two paths can be used as an error detecting metric. Obviously this error detection metric will depend on the noise

present in the channel. As the channel conditions become worse the error detection metric decreases. Under very bad channel conditions this metric will fall to zero. This means the decoded bits are totally unreliable. Fig. 3.15 gives the probability density function of the mean error detection metric at the output of the decoder for the (16,5,8) GAC for channel signal to noise ratio 2, 4, 6, and 8, and for the (16,11,4) GAC codes for SNR 5,6,7 and 9dB, each for 100 000 blocks transmitted. It can be seen that the means are quite distinct. Figs. 3.16 shows the variation of the mean error detection metric and their standard deviations for the (16,5,8) and for the (16,11,4) GAC codes with respect to the channel SNR. These figures indicate that this error detection metric is a good indication of the level of noise in the channel. Since the error probability of the trellis decoders depend on the channel signal to noise ratio an estimate of the output probability of error from the decoder of each of the three codes are obtained once the SNR of the channel is determined. The statistical channel evaluator or error limiter averages the error detection metrics over a certain number, b , of blocks, where b depends on the standard deviation of the error detection metric about its mean. This average is compared with a set of previously determined thresholds carefully selected in order to limit the error probability below a certain maximum specified level.

Fig. 3.15(i) PDF vs Error Detection Metric of the (16,5,8) GAC code

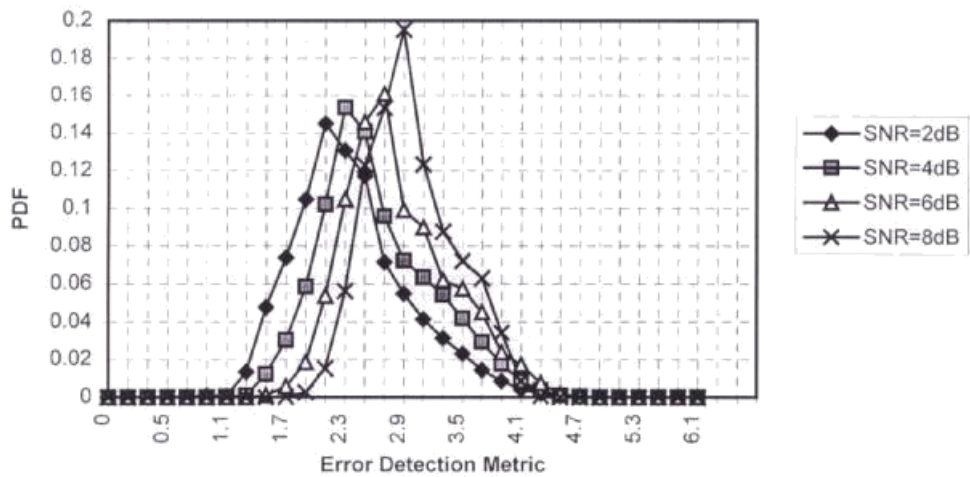


Fig. 3.15(II) PDF vs Mean error detection metric for the (16,11,4) GAC code

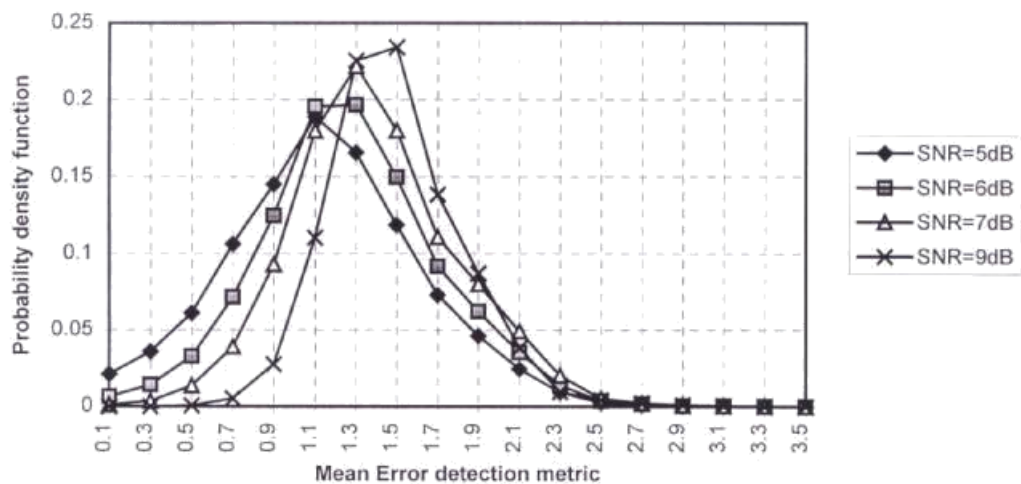


Fig. 3.16(i) Mean error detection metric vs SNR for the (16,5,8) GAC code

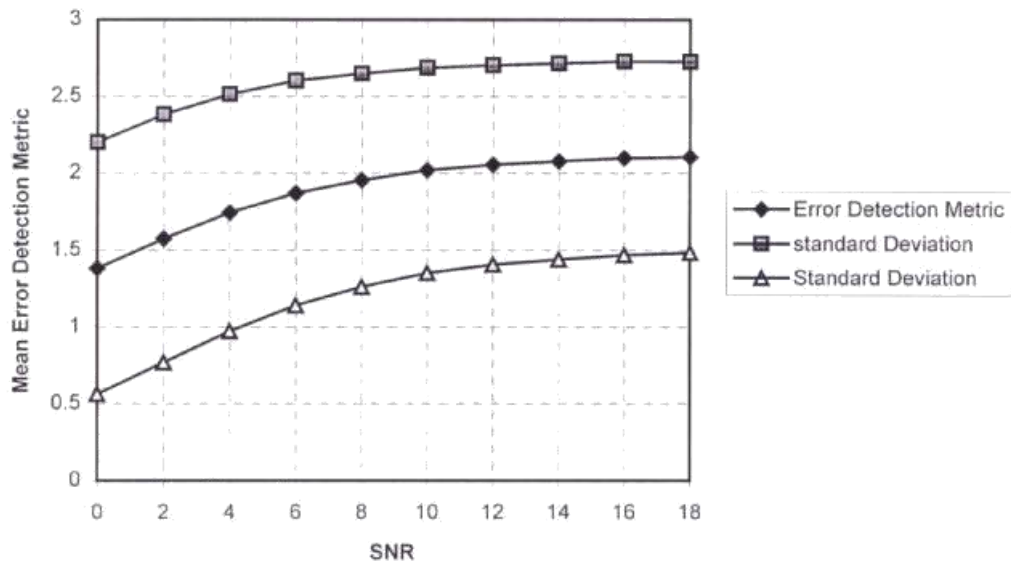
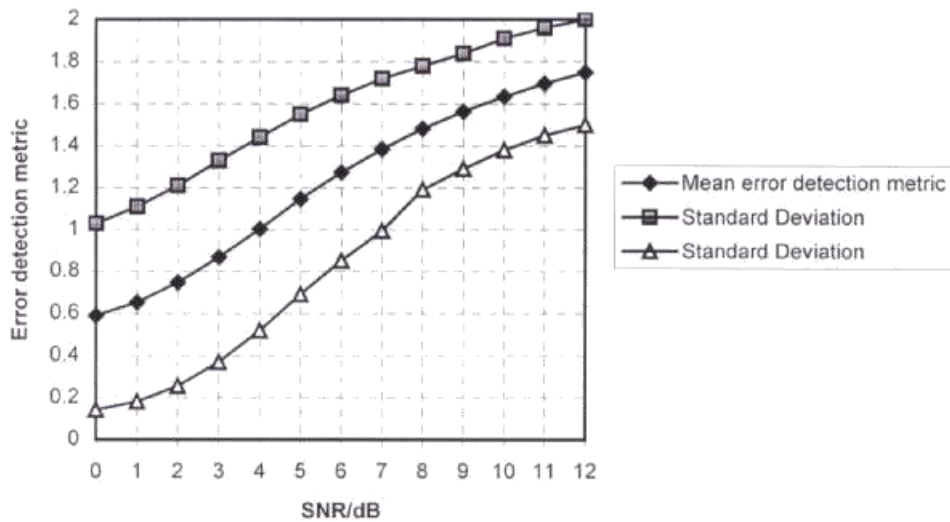


Fig. 3.16(ii) Mean error detection metric and its standard deviation for the (16,11,4) GAC code



3.6 Simulation Results and Discussions

The simulation tests were carried out under slow Rayleigh fading and AWGN channel conditions. The results presented here are for BPSK signalling scheme. For all cases perfect bit and block synchronisation are assumed. The effect of the channel SNR on the BER of the component codes has been illustrated in Figs. 3.10, 3.17 and 3.18 respectively give the reliability and the throughput efficiency of the embedded code and the (16,11,4) component code. As can be seen from these figures the embedded code gives a higher reliability than the (16,11,4) GAC code and that the embedded code gives a higher throughput than the (16,11,4) GAC code for Channel BER above 8×10^{-2} . Fig 3.19 shows that the embedded code gives a higher throughput than the (16,11,4) GAC code below 12 dB. The disadvantage of this modified embedded code proposed is that the decoder requires three different trellises, one for each component code. Hence another embedded code has been designed that employs the same trellis in a nested fashion to decode all the three component codes in the embedded block.

Fig. 3.17 Output BER vs Channel BER for embedded code and (16,11,4) GAC code

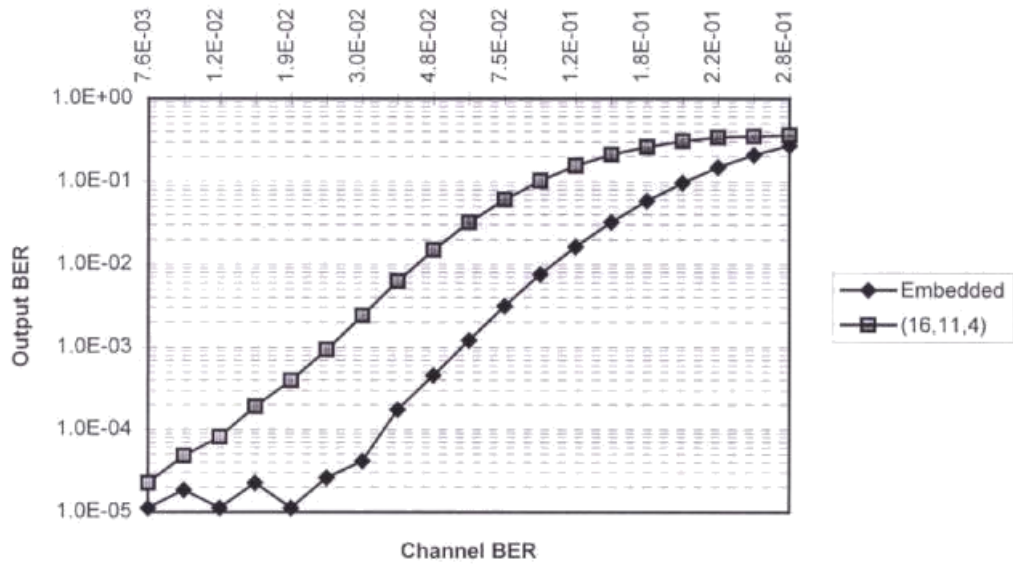


Fig. 3.18 Throughput vs channel bit error rate for embedded code and (16,11,4) GAC code

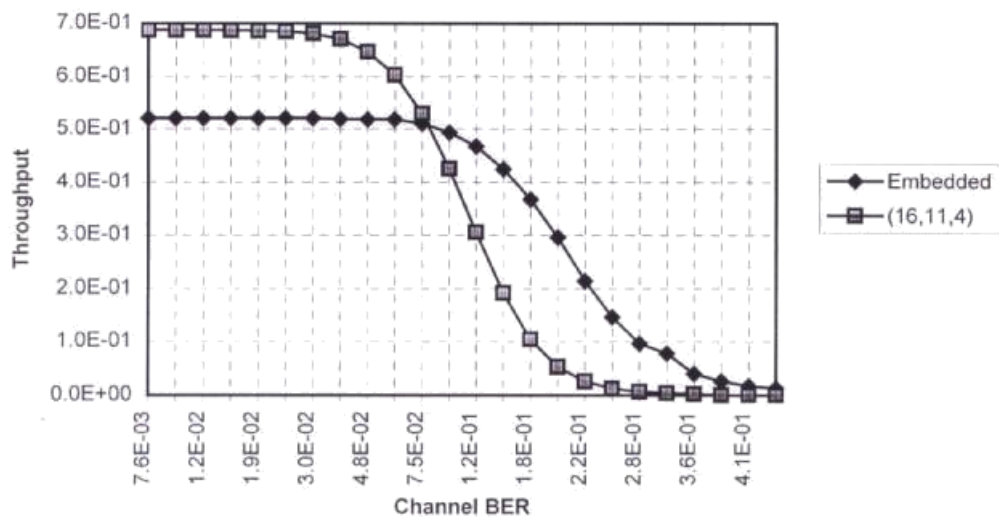
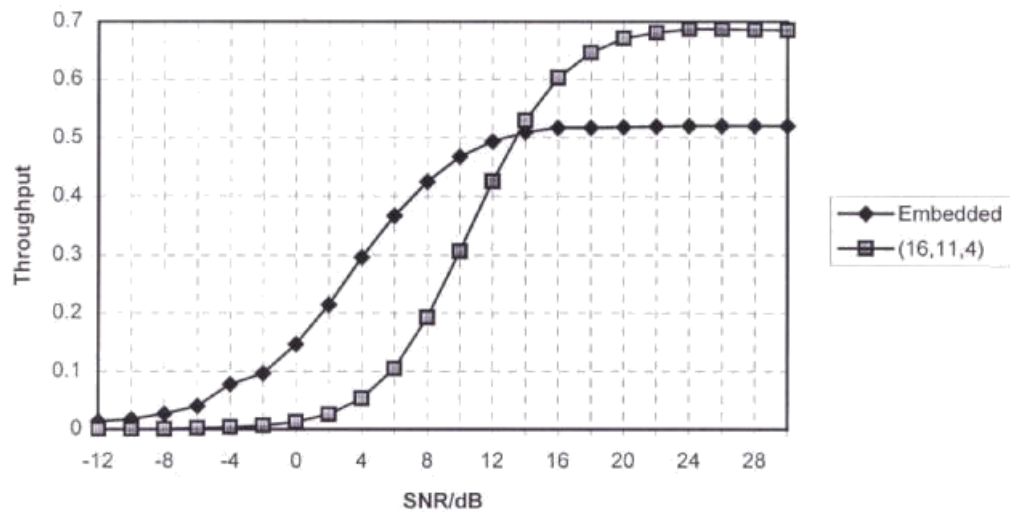


Fig. 3.19 Throughput vs SNR for embedded and (16,11,4) GAC code



3.7 Embedded Code employing Linear Block Codes and Nested Trellis Decoding.

The new embedded code [Soyjaudah and Honary 1997] employs GAC codes, whilst retaining the desirable reliability performance of the embedded codes. The main block comprises three streams, each encoded independently using the codes C_1 , C_2 , and C_3 that are respectively the (32,6,16), (16,5,8) and the (8,4,4) GAC codes and are given by:

$$c_1 = \begin{bmatrix} x_1 & x_1 \oplus x_4 & x_1 \oplus x_5 & x_1 \oplus x_4 \oplus x_5 & x_1 \oplus x_6 & x_1 & x_1 & x_1 \\ x_2 & x_2 \oplus x_4 & x_2 \oplus x_5 & x_2 \oplus x_4 \oplus x_5 & x_2 \oplus x_6 & x_2 & x_2 & x_2 \\ x_3 & x_3 \oplus x_4 & x_3 \oplus x_5 & x_3 \oplus x_4 \oplus x_5 & x_3 \oplus x_6 & x_3 & x_3 & x_3 \\ p_1 & p_1 \oplus x_4 & p_1 \oplus x_5 & p_1 \oplus x_4 \oplus x_5 & p_1 \oplus x_6 & p_1 & p_1 & p_1 \end{bmatrix}$$

$$c_2 = \begin{bmatrix} x_1 & p_1 \oplus x_4 & p_1 \oplus x_5 & p_1 \oplus x_4 \oplus x_5 \\ x_2 & p_2 \oplus x_4 & p_2 \oplus x_5 & p_2 \oplus x_4 \oplus x_5 \\ x_3 & p_3 \oplus x_4 & p_3 \oplus x_5 & p_3 \oplus x_4 \oplus x_5 \\ p_4 & p_4 \oplus x_4 & p_4 \oplus x_5 & p_4 \oplus x_4 \oplus x_5 \end{bmatrix}$$

$$c_3 = \begin{bmatrix} x_1 & x_4 \oplus p_1 \\ x_2 & x_4 \oplus p_2 \\ x_3 & x_4 \oplus p_3 \\ x_4 & x_4 \oplus p_4 \end{bmatrix}$$

The coderates are $\frac{6}{32}$, $\frac{5}{16}$ and $\frac{4}{8}$ and they possess decreasing error correcting capability. The structure of the embedded code is shown in Fig.3.20.

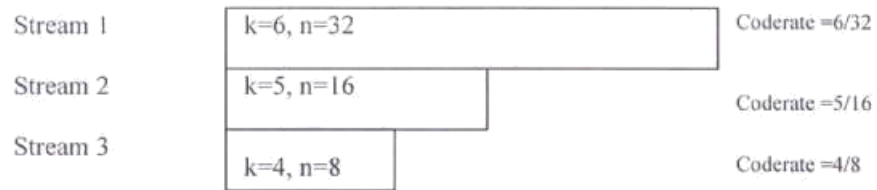


Fig. 3.20. Structure of embedded code based on GAC codes

The overall system is the same as shown in Fig. 3.5. The differences are that no outer code is used and that only one nested trellis is used to decode all the components of the embedded code. The transmitter and receiver operate at baseband using bipolar signalling. The transmitted levels are set at +1 and -1 volts, corresponding to binary digits 1 and 0 respectively.

The encoding is performed as follows:

- (i) A message of 15 bits is divided into three information sub-blocks {6,5,4}
- (ii) Each sub-block is then encoded in a manner described above depending on its position in the main block using the generalised array codes C_1 , C_2 , and C_3 . These resulting sub-blocks are then transmitted. The channel is slow Rayleigh fading and introduces AWGN with a mean of zero and a standard deviation of σ . The decoder comprises two main elements, soft decision maximum likelihood trellis decoders for the decoding of the GAC codes and an error limiter. Since the trellis structure of the three codes are similar the error correction within the sub-blocks C_1 , C_2 , and C_3 is realised by using a single trellis in a nested fashion. The structure of this nested trellis

is given in Fig. 3.21. The error limiter operates in the same way as described in section 6.5.3 and limits the output error probability of the overall system.

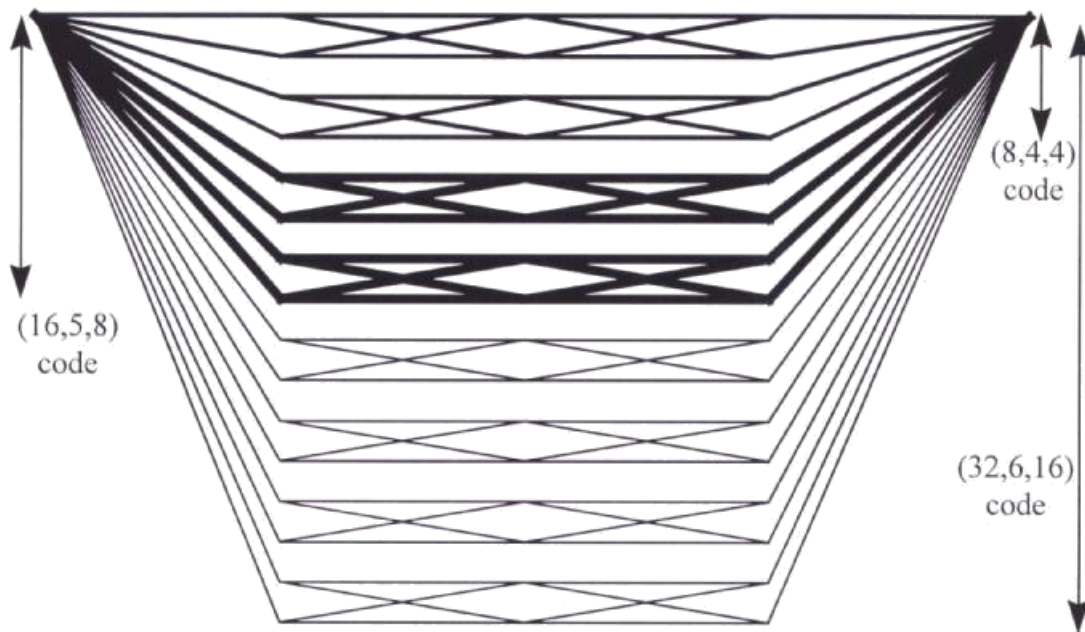


Fig. 3.21 Nested trellis of (32,6,16), (16,5,8) and (8,4,4) GAC codes.

3.8 Simulation Results and Discussions

The simulation tests were carried out as in the other cases under slow Rayleigh fading and AWGN channel conditions. The results presented are for bipolar signalling scheme assuming perfect bit and block synchronisation during transmission. Fig 3.22 shows the effect of the channel SNR on the BER of the three linear block components codes. Suppose we wish to use the embedded codes for transmission when the error rate exceeds 10^{-2} . It can be seen from Fig. 3.22 that none of the codes C_1 , C_2 , and C_3 will be accepted until the SNR exceeds about 0 dB. C_1 is accepted beyond about 0 dB

while C_2 and C_3 are respectively accepted beyond about 2.0 and 8 dB respectively. Figs. 3.23 and 3.24 respectively give the reliability and the throughput efficiency of the codes. Fig. 3.25 gives the variation of the throughput with SNR for the embedded code and the (8,4,4) code. Comparison of the embedded code and the (8,4,4) component code shows that the embedded encoding method yields a high reliability at very high bit error rates (for example at a BER of 0.05). Although for low channel BER (below 0.05) the throughput efficiency of the embedded technique is greatly reduced due to the redundancy of the code C_1 , for high channel BER (above 0.05), the embedded system gives an improved throughput. In the above discussions, fixed transmission rates (Baud rates) for both the embedded code and any component linear block code has been assumed. It is clear that if the transmission rate of the linear block codes is reduced so that the error-free throughputs of the two codes are the same, the reliability of the component codes would be superior to that of the embedded code. However the component code would cease to operate effectively at a channel BER greater than 0.05, while the embedded code would continue to perform successfully under such conditions.

Fig. 3.22 Output BER vs SNR

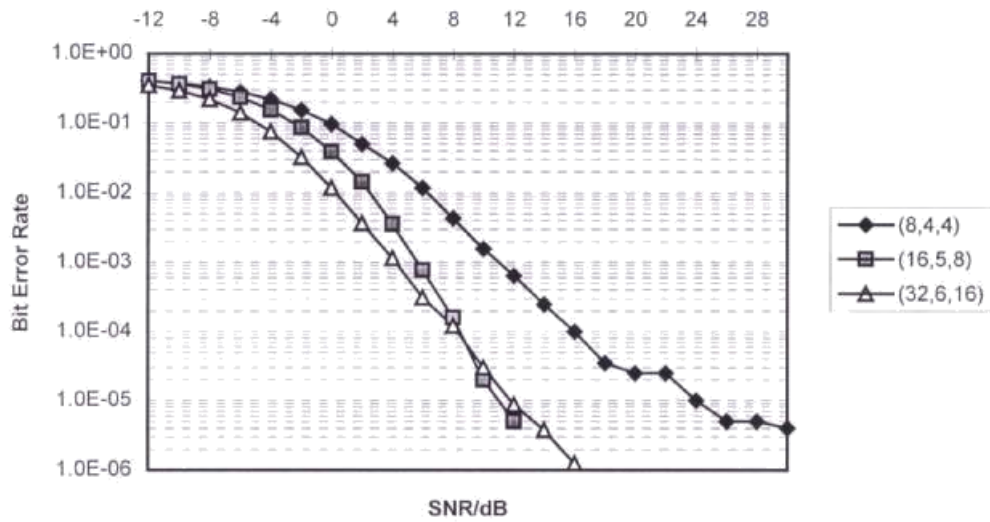


Fig. 3.23 Output BER vs Channel BER

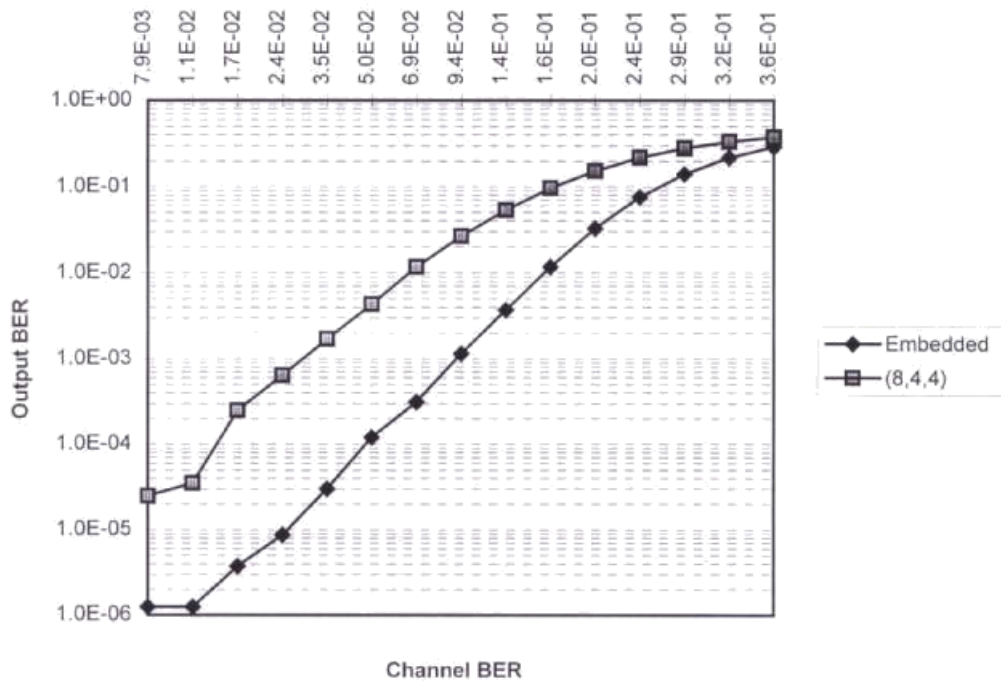


Fig. 3.24 Throughput vs Channel BER

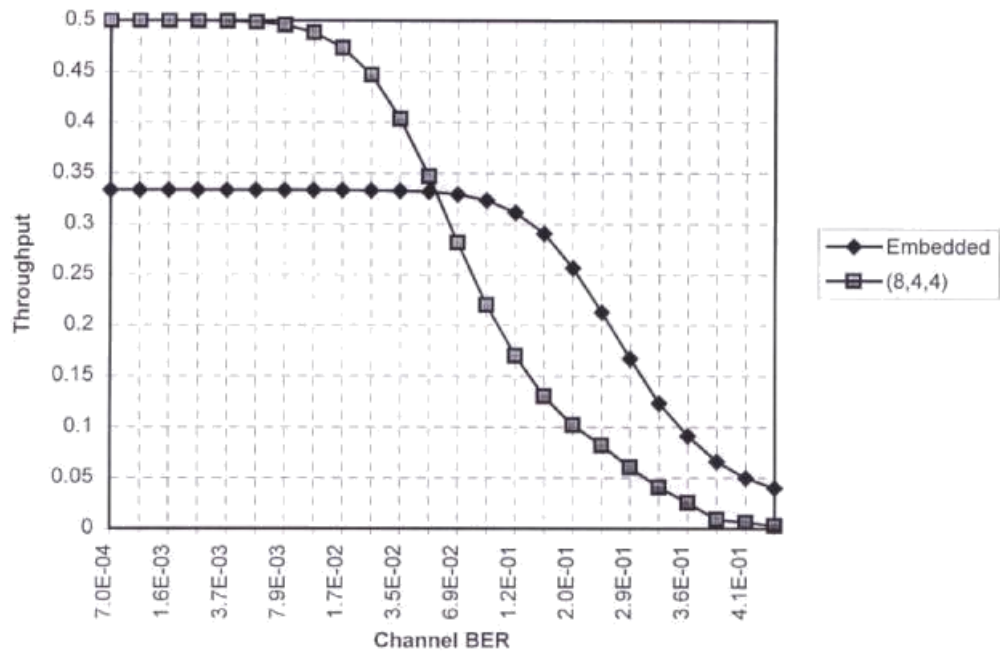
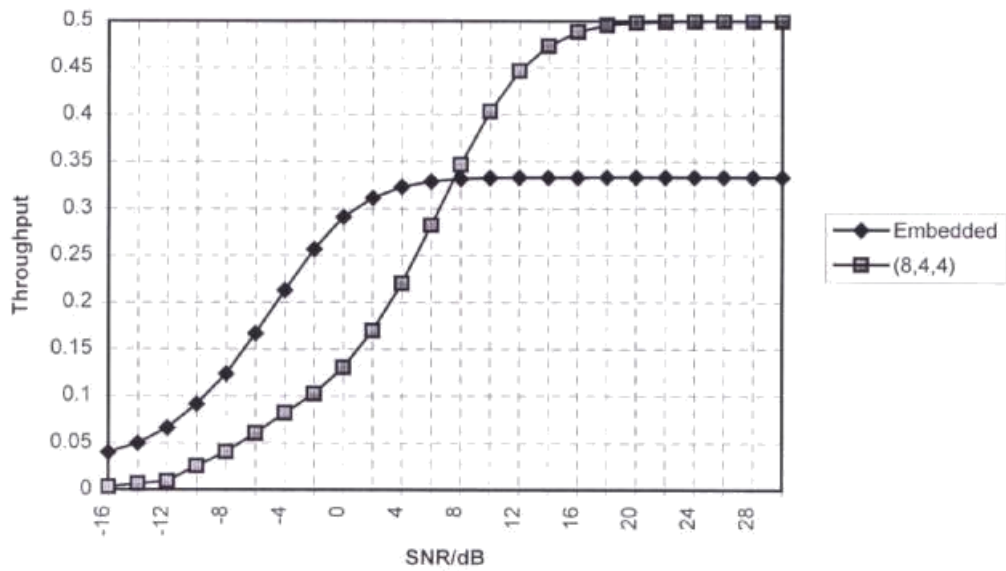


Fig. 3.25 Throughput vs SNR



Chapter 4

Trans-Equatorial Link Between Mauritius and Europe

1. Introduction

Signal transmissions in the high-frequency (HF) band (2-30 MHz) can propagate by a number of different mechanisms (including ground wave, single and multi-hop skywave, sporadic-E etc). The various propagation mechanisms and other ionospheric effects can result in the signal suffering multipath dispersion, Doppler shifts and Doppler spreading (frequency dispersion) and attenuation. Whilst these effects occur all over the World, there is a particular interest in the trans-equatorial, where very severe Doppler spreads and multipath dispersion occur. A survey of propagation literature has shown that little data exists which provides information on the magnitude and frequency of occurrence of multipath dispersion and Doppler spread over these trans-equatorial paths. Available data suggests that Doppler spread may be encountered for substantial percentages of the time.

One of the most important objectives of establishing the link is to statistically quantify spectral spreads, Doppler shifts, multipath delay and signal strengths for a trans-equatorial paths. This is to be achieved by collecting a large database of measurements over a period of many months. This data provide much of the basic information required to fulfil the project's other major objectives, namely the testing of improved source and channel coding, modulation and networking techniques.

2. MEASUREMENT SYSTEM

The measurement system employs an oblique channel sounding system which has been developed the UK Defence Research Agency (DRA) to measure a number of real-time channel parameters

using low power pulse compression waveform transmissions. This system is called DAMSON (Doppler And Multipath SOunding Network). Extensive use is made of digital signal processing techniques. The system will allow signal time-of-flight, time dispersion (multipath dispersion), frequency dispersion (Doppler spread and Doppler shift) and signal strength to be measured over point-point communications paths

The DAMSON system uses relatively low power coded transmissions between remote transmit and receive sites on a pre-selected range of frequencies to determine the following real time oblique channel parameters:

1. Absolute time of flight
2. Multipath dispersion
3. Doppler shift & spread
4. Signal strength
5. Signal to noise ratio

The system determines channel parameters using pulse compression sounding waveforms to increase the total energy available at the receiver, by increasing the transmission time, whilst maintaining the time resolution that could be obtained from a single pulse (equivalent to the compressed pulse width). Timing resolution is determined by the system bandwidth, normally either 3 kHz or 12 kHz, which limits the minimum pulse width through the system. Pulse compression and integration over many pulses yields typical signal processing gains of ~ 35 dB (depending on the particular waveform in use).

The system is based on commercially available equipment (such as HF communications receivers, computers etc) and makes extensive use of Digital Signal Processing (DSP) techniques. High accuracy system timing is derived from the constellation of Navstar Global Positioning

System (GPS) navigation satellites. This ensures that transmit and receive stations are accurately synchronised and also allows absolute time-of-flight measurements to be made.

It is not possible to measure all the channel parameters over the required ranges using a single waveform; some of the requirements are quite contradictory. In order to increase the performance and flexibility of the system, and in the light of these constraints, the particular waveforms in use and their characteristics (type, duration, bandwidth, pulse repetition frequency (PRF), number of pulses etc) are all specified in a configuration file. Hence the waveform in use can be tailored to the particular measurement being made. The principal constraint on this flexibility is that waveform parameters must be pre-arranged between transmit and receive stations. The system has been designed to support a wide range of different pulse compression waveforms including, in particular, a variety of PSK modulated sequences (including Barker sequences, maximal length pseudo noise (PN) sequences and complementary sequences) as well as linear FM chirps, up-down chirps etc.

Measurements are made using a combination of four basic modes:

1. Time of flight (TOF) search mode
2. Delay Doppler (DD) measurement mode
3. CW measurement mode
4. Noise measurement (NM) mode

The time-of-flight (TOF) mode is used to determine both the basic signal time of flight and approximate multipath profile while the Delay-Doppler (DD) mode determines the channel multipath profile, Doppler spread and Doppler shift. Both modes can also collect signal strength information. Two additional measurement modes will be implemented. A CW measurement mode will allow the receiver gain to be automatically adjusted if required and then used to determine large frequency shift/dispersion conditions (useful for data 'pre-screening'). A noise-

monitor (NM) mode will be used to determine the quiescent channel conditions (interference etc.) for accurate signal-to-noise calculation etc.

The following measurement schemes are supported:

1. Fixed Frequency operation. Allows the investigation of a single frequency (or a number of specified frequencies). Typically the system would determine the signal TOF, multipath dispersion, Doppler spread and signal strength for a frequency using the TOF search mode followed by the DD measurement mode.
2. Scanning Ionogram operation. The system steps through frequencies (across all or any part of the HF band) sounding channels to produce a conventional type ionogram together with TOF and Doppler information as required.

The DAMSON system software includes scheduler routines which allow measurement schemes to be repeated at selected intervals over any chosen time period.

By analysing data collected over a period of time the changing nature of the channel can be investigated. The instrument allows information on the frequency of occurrence and severity of time and frequency dispersion over different paths (especially high latitude and trans-auroral paths), diurnal and seasonal variations and the effect of ionospheric disturbances to be collected.

3. TRANSMIT STATION CONFIGURATION

A DAMSON transmit station, Fig.4.1, consists of an IBM compatible personal computer (PC) which is used to perform basic system control functions. Plugged into the PC is a DSP card which carries out both the real time processing and the digital to analogue conversion required to accurately generate waveforms and trigger their transmission. The baseband output of the DSP sub-system drives the modulation input of a HF single-sideband (SSB) drive unit. Basic transmit parameters such as frequency and transmit bandwidth are controlled by the PC via a serial communications interface. The HF drive has a high stability frequency reference (better than 1 in

10⁶) and a number of software selectable SSB bandwidths including a maximum bandwidth of 12 kHz. The HF drive unit output is fed to a wide-band linear power amplifier which in turn feeds a maximum power of between 500 W and ~1 kW into the antenna system. For fixed operation on long or difficult paths it is envisaged that a (calibrated) directive antenna aimed at the receive site be used. System timing and hence synchronisation with the receive station is obtained from a GPS receiver card plugged into the PC.

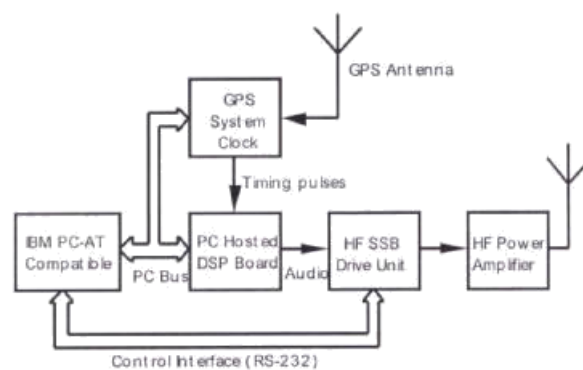


Fig.4.1 Configuration of Transmit System

HF transmitters are located at Farnborough and Cobbett Hill in UK and at Harstad in Norway. The Cobbett Hill HF transmitter antenna is located at 51.27° North and 0.8° West. This is a directional transmitter of high power (1000w) and has an antenna gain of 8dB. The transmission frequencies from this station are 9224.5, 12194.5, 15961.5, 18188. 20121.5, and 23759.5 kHz and these frequencies have been allocated by mutual agreement by the Mauritian and British authorities. The transmitter at Harstad is under remote control using a modem link

4. RECEIVE STATION CONFIGURATION

The receive station, Fig.4.2, consists of a receive antenna system, a good quality HF communications receiver and a signal processing and data storage/analysis system. The receiver is fully software controllable using a serial control interface. It has a high quality stable oscillator (better than 1 in 10^6) and a one Hertz tuning accuracy. The receiver baseband output is fed to the analogue to digital converter (ADC) input of the DSP card. The receiver can be operated in either an automatic gain control (AGC) mode or in a manual (computer controlled) IF gain mode to allow more accurate signal strength and fading measurements to be made.

A PC is used to perform basic system control functions, data archiving, analysis and display. Plugged into the PC is a DSP card which both samples the received signal, using an on-board ADC, and carries out all the real time processing required to detect and process received transmissions. Sampling is performed at twice the Nyquist rate to allow in-phase and quadrature (IQ) processing of the received signals. As with the transmitting station system timing is obtained from a GPS receiver card plugged into the PC.

Measurements made using the DAMSON system contain a large amount of data (upto ~50 kbytes for a 5 s measurement). This is initially stored to a large hard disk (One giga-byte capacity) and then periodically archived to digital audio tape (DAT).

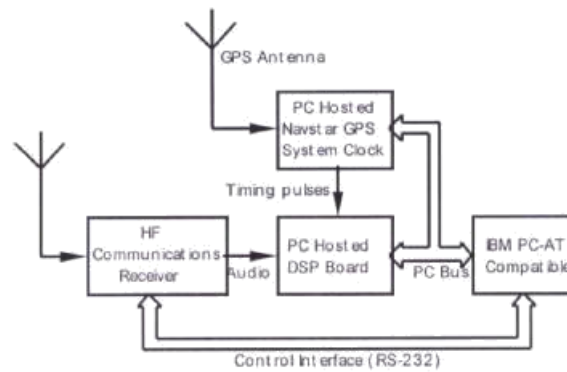


Fig.4.2 Receive Station Configuration

Fig. 4.3 gives the location of the receive HF antenna location. As can be observed the HF mast which is 18 metres high is located on the roof of the Textile building. The HF antenna Fig. 4.4 which is V-shaped starts on the mast 1 metres below its top and terminates on the roof of the mechanical workshop Phase1. The antenna wires are separated by a distance of 40 metres on the roof of the mechanical workshop. Each has a terminating resistor of $300\ \Omega$ that ends with an earth rod 8 metres into the ground. Also the antenna wires are linked together with a thick copper wire at the terminating end.

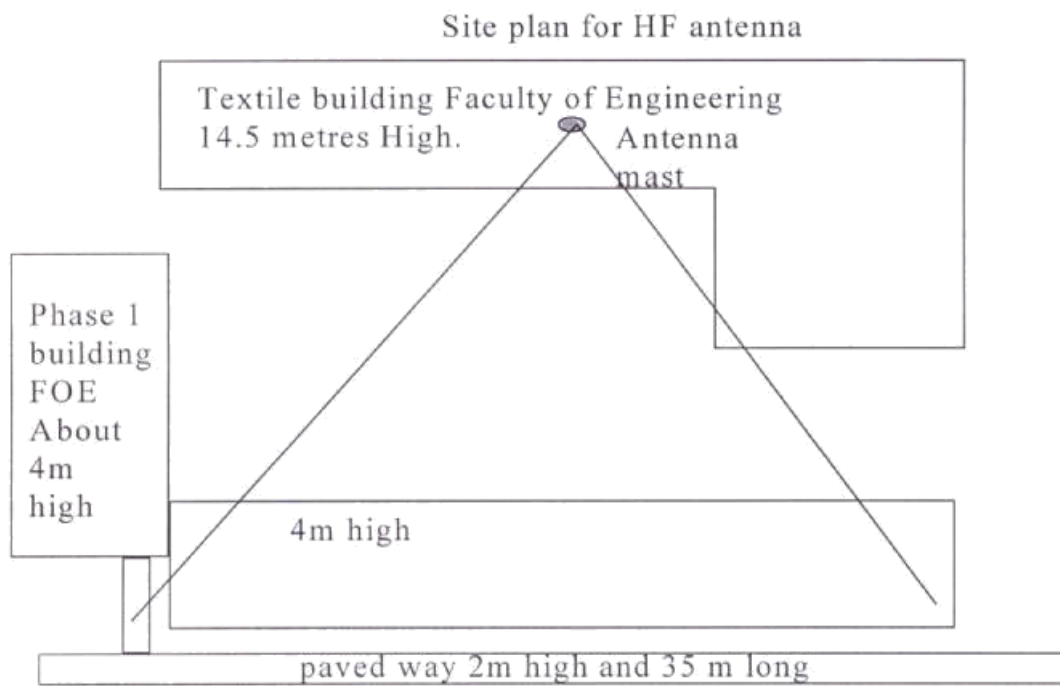


Fig.4.3 Location of the HF receive antenna

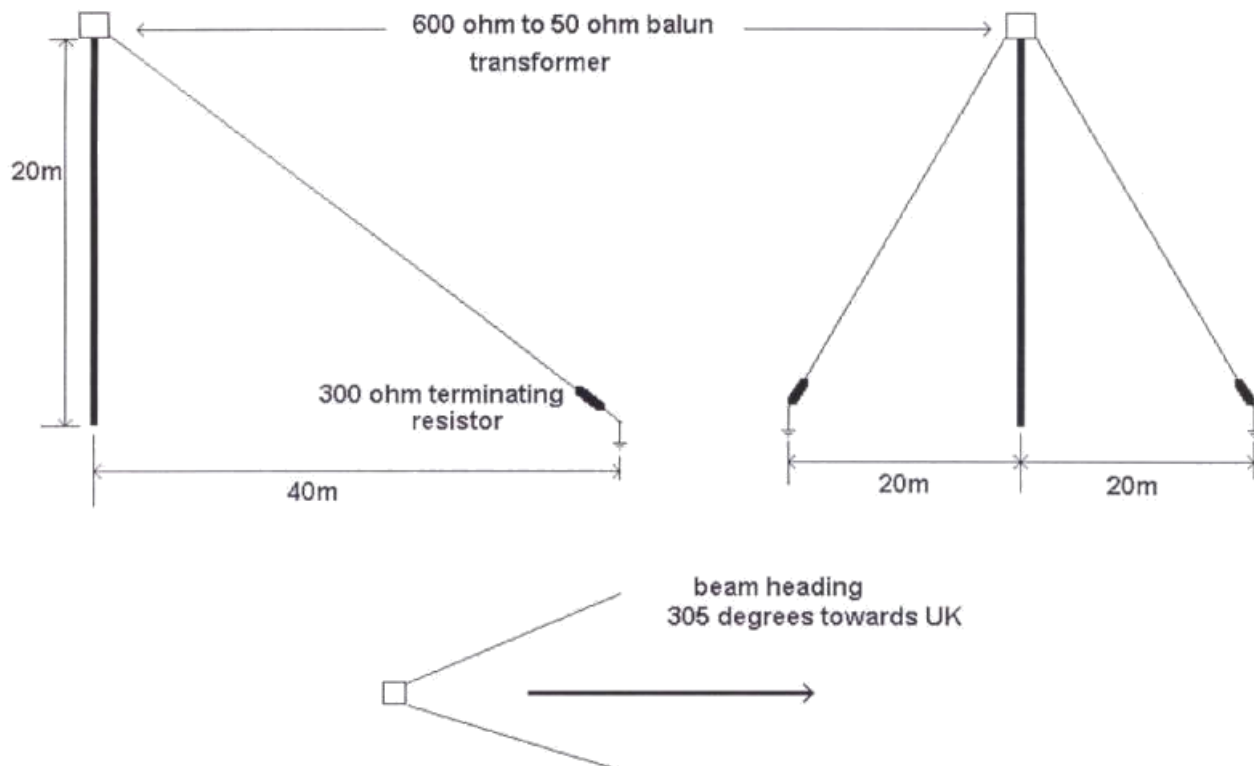


Fig.4.4 HF receive antenna

5. TIME OF FLIGHT SEARCH MODE

In this mode the transmit station sends a number of accurately timed pulse compression waveforms in order to allow the receive station to determine the basic signal propagation delay (TOF) and a low resolution picture of the multipath structure. The principle requirement in this mode is for a waveform that gives good signal detectability in the presence of delay and Doppler dispersion rather than highly accurate time-of-arrival. A typical waveform for use in this mode is a bi-phase PSK modulated Barker-13 sequence which gives reasonably good detectability whilst being short enough to be robust in the presence of fading. In order to cater for all envisaged paths with no time (range) ambiguity, a pulse repetition interval (PRI) longer than the maximum anticipated TOF is required (up to at least 100 ms for longer paths). In order to increase the total energy available at the receiver the waveform is transmitted a number of times. The received pulses are detected and Doppler integrated (see section 6) to determine the basic TOF from the time-of-arrival and knowledge of the transmission time (accurately determined from the GPS timing source). In addition this mode will provide a low resolution picture of the multipath dispersion.

6. DELAY DOPPLER MEASUREMENT MODE

This mode is used to determine the detailed multipath dispersion and Doppler characteristics of a channel once the TOF search mode has been used to identify the approximate time window during which the received signals arrive. The transmit station sends a number of accurately timed pulse compression waveforms in order to allow the receiving station to determine multipath dispersion, frequency dispersion (Doppler spread and Doppler shift) and received signal strength. Principal requirements of a pulse compression waveform to be used in the DD mode is that it gives good time resolution (approaching the maximum for a given channel bandwidth), has a

large dynamic range (peak-sidelobe ratio) and that it performs adequately in a frequency dispersive environment (a non time coherent channel will generally reduce the observed peak-sidelobe ratios). Suitable pulse compression waveforms include BPSK modulated Barker sequences, periodic maximal length PN sequences and complementary sequences. The nominal peak-sidelobe performance of the latter sequences are excellent but degrade quickly in the presence of fading and changing channel phase.

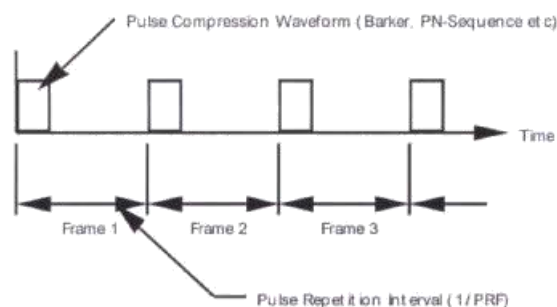


Fig.4.5 Transmitted Waveform Frame Structure in Delay Doppler (DD) Measurements Mode

The pulse compression waveform is sent many times (typically 64, 128 or 256 times), the interval between the start of each waveform transmission being termed a frame as shown in Fig.4.5. The period of a frame determines the multipath measurement time 'window'. If pulse-to-pulse coherence is maintained for the transmitted signal any spectral spreading/frequency shifts observed at the receiver will be due to ionospheric effects.

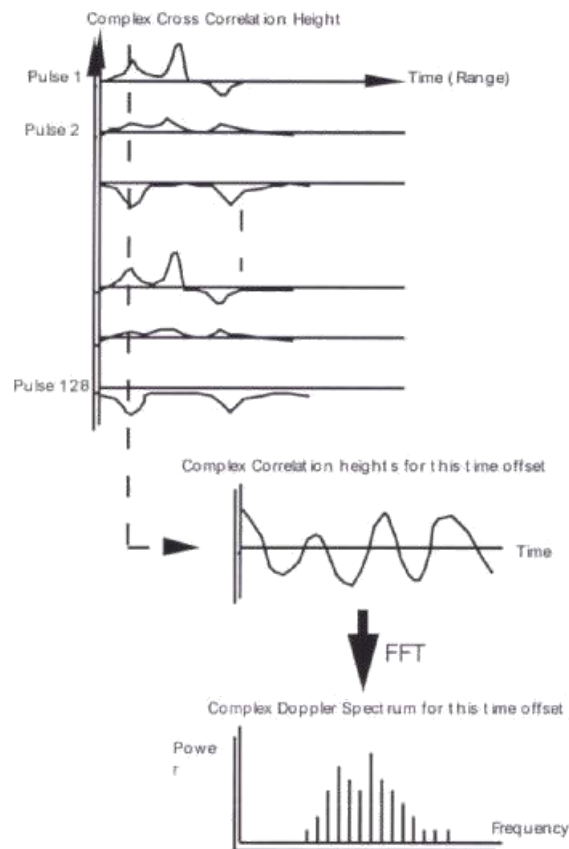


Fig.4.6 -Calculation of Doppler Spectra for Each Time Delay Interval Using Doppler Integration

The receiver detects the pulse compression waveform by continuously sampling the receiver output, converting the received signal to IQ and cross correlating it against a complex unit template of the pulse compression waveform transmitted. This process gives a complex cross-correlation height for each time offset (range). The output of the cross-correlator over the period of one frame is the complex channel impulse response as in Fig.4.6. If the channel caused no frequency dispersion then the impulse response for each frame would be identical. However in the more general case fading would cause the received energy to be dispersed between the in-phase and quadrature channels ,as shown in Fig.4.6, top left.

Once the complex impulse responses have been calculated for all the transmitted frames then the system can calculate the Doppler spectra for each time offset in the multipath window. This is done by making a time series of the complex cross-correlation heights at the same time offset in the multipath window for each successive frame and then taking its Fourier transform using a Fast Fourier Transform algorithm (FFT) to obtain the Doppler spectra for that time offset. The total power in the spectra is the received energy at that time offset integrated across all the received waveforms (Doppler integration). Hence the multipath profile, as measured by the system, is the total energy in the Doppler spectra for each time-offset plotted against its time offset.

The DAMSON system can thus determine both the channel multipath profile and the frequency spectra (Doppler shift and spread) for each received mode.

The maximum timing resolution possible is determined by the system bandwidth. Using a system bandwidth of 12 kHz and a 9600 baud PSK waveform would give a multipath dispersion resolution of $\sim 100 \mu\text{s}$ (digitising resolution $25 \mu\text{s}$). The multipath time period (range or multipath 'window') that can be investigated unambiguously is determined by the frame period. Larger multipath spreads than the frame period will cause interference in subsequent frames. The Doppler frequency range for a DD measurement is also determined by the frame period; it is $\pm(\text{PRF}/2)$, the PRF being $1/(\text{frame period})$. The presence of larger Doppler frequencies than this will cause aliasing and appear as lower frequencies within the measurement range. The unambiguous multipath and Doppler ranges that can be measured simultaneously must be traded off; as the unambiguous multipath range increases the Doppler range decreases. Hence compromises have to be made in choosing the measurement parameters. The Doppler resolution of the system is directly proportional to the total integration period (i.e. total receive time). An integration period of one second would give a resolution of 1 Hz whereas an integration time of 0.5 s would give a resolution of 2 Hz etc. Table 4.1 shows the trade-offs between Delay Range, Doppler range/resolution and total measurement time (maximum signal integration period).

Delay Range (ms)	Number of Frames	Doppler Range (Hz)	Doppler Resoluti on (Hz)	Integra tion Period (s)
5	64	± 100	3.12	0.32
5	128	± 100	1.56	0.64
5	256	± 100	0.78	1.28
5	512	± 100	0.39	2.56
10	64	± 50	1.56	0.64
10	128	± 50	0.78	1.28
10	256	± 50	0.39	2.56
10	512	± 50	0.19	5.12
15	64	± 33	1.04	0.96
15	128	± 33	0.52	1.92
15	256	± 33	0.26	3.84

Table.4.1 - Trade-offs between Delay Range, Doppler Range/Resolution and total DD Measurement Time (3 kHz bandwidth and 9600 samples per second)

Results and discussions

Data transmitted from Scandinavian and British transmitters have been recorded employing the receiver in Mauritius. Most of the signals received from Scandinavian sources were very noisy. Fig. 4.7 gives a good measurement data transmitted from a transmitter in Scandinavia situated at

70.0° north and 5.0° East on 24 September 1997 at 12:20:47 hours. The received mode as a hump with a time of flight just under 40 ms can clearly be seen. The multipath profile indicates that the transmission is through a single hop. The CW measurement indicates that the signal has undergone quite a large amount of frequency shift. The frequency spread is 12.89 Hz in this case. The noise monitor measures the mean noise as 1476 and enables the SNR to be measured as -15.27 dB. This shows that the channel is very noisy. Figs. 4.8-4.10 give correctly received Damson pictures transmitted from Guildford on 13 May 1998 between 11.00 and 12.00 hours.

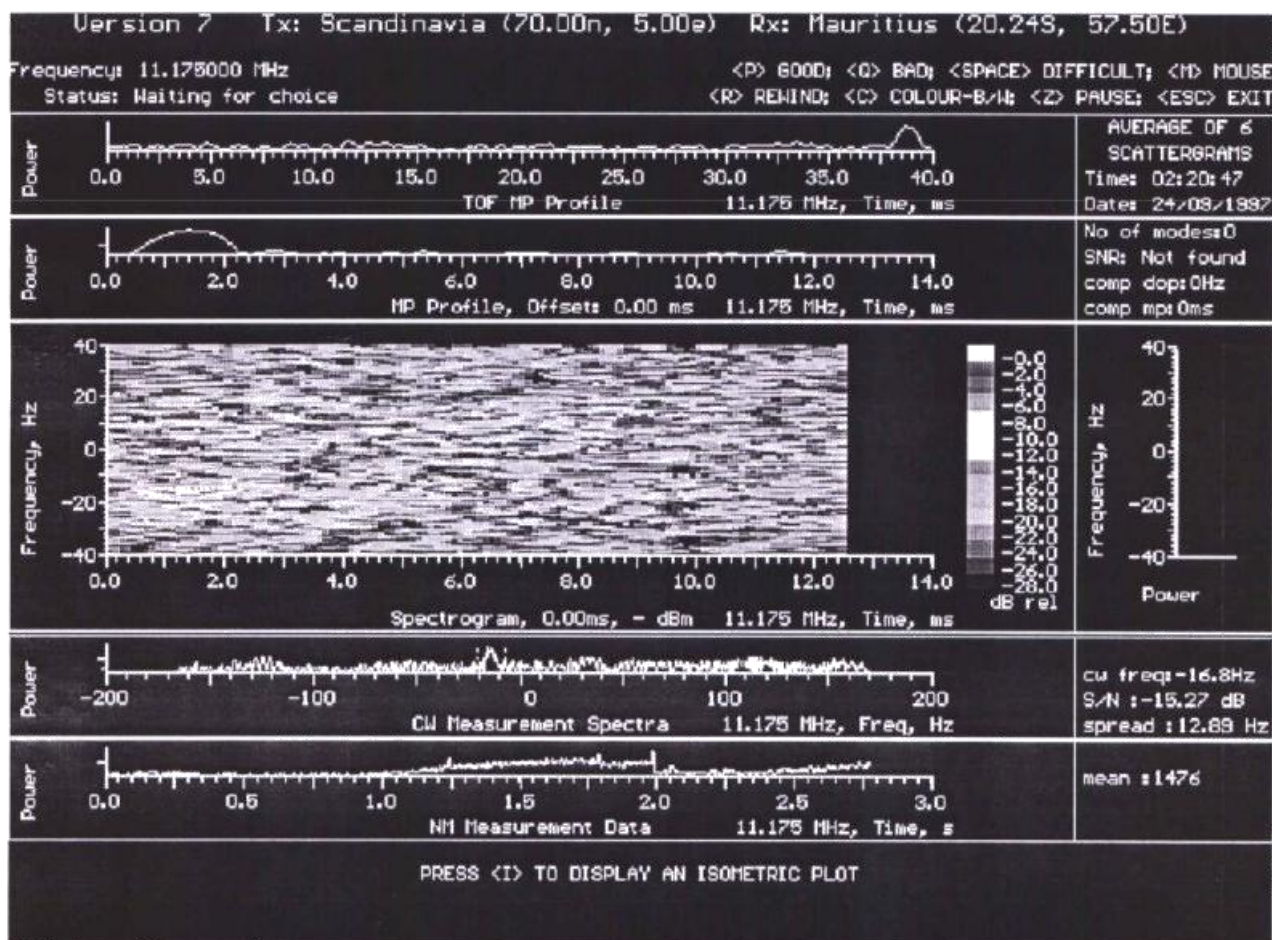


Fig. 4.7 Data received from transmitter in Scandinavia situated at 70.0° North and 5.0° East.

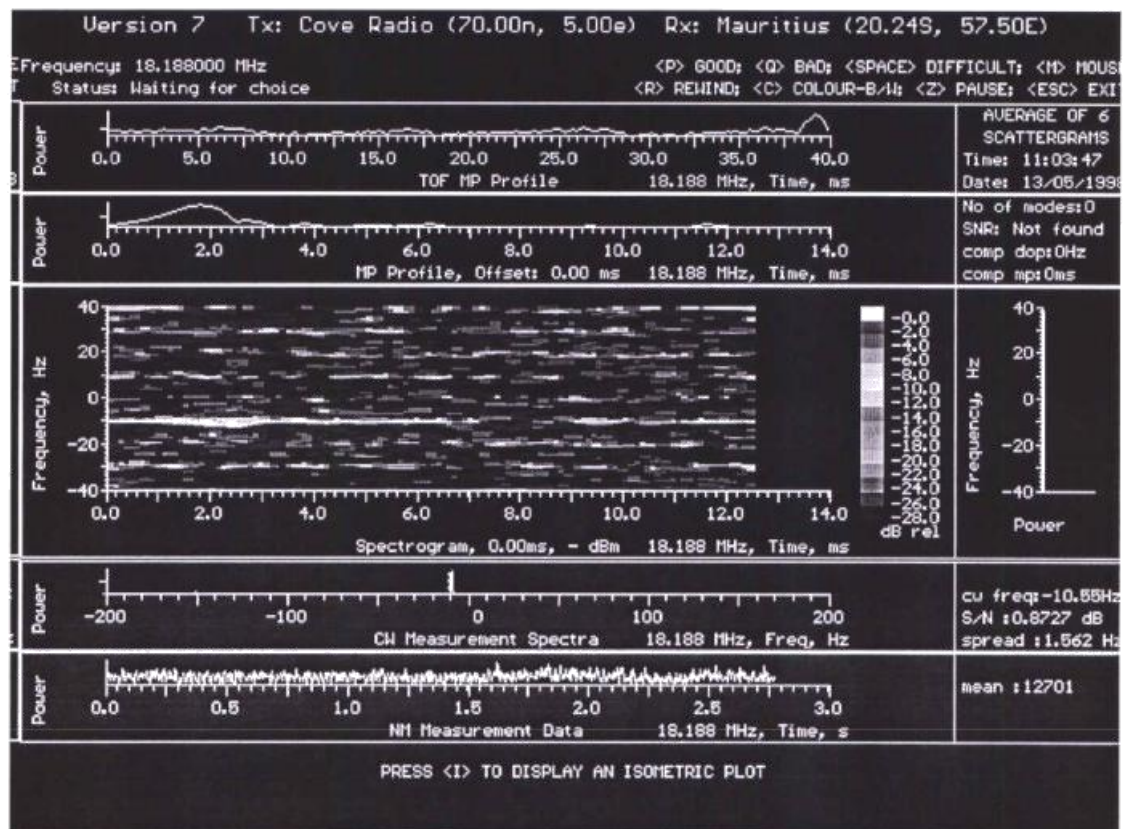


Fig. 4.8 Data from Guildford transmitting at a frequency of 18.188 MHz

The received mode as a hump with a time of flight just under 40 ms can clearly be seen from these figures. The multipath profile shows that each of these signals are received as a single hop signal. The spectrograms give the corresponding strength of received signals. The CW measurement in this case indicates the frequency spread is much less than 2 Hz in these cases. The noise monitor enables the average noise to be estimated and the corresponding SNR to be evaluated. It is seen the received signal is much less noisier than those received from Scandinavian sources.

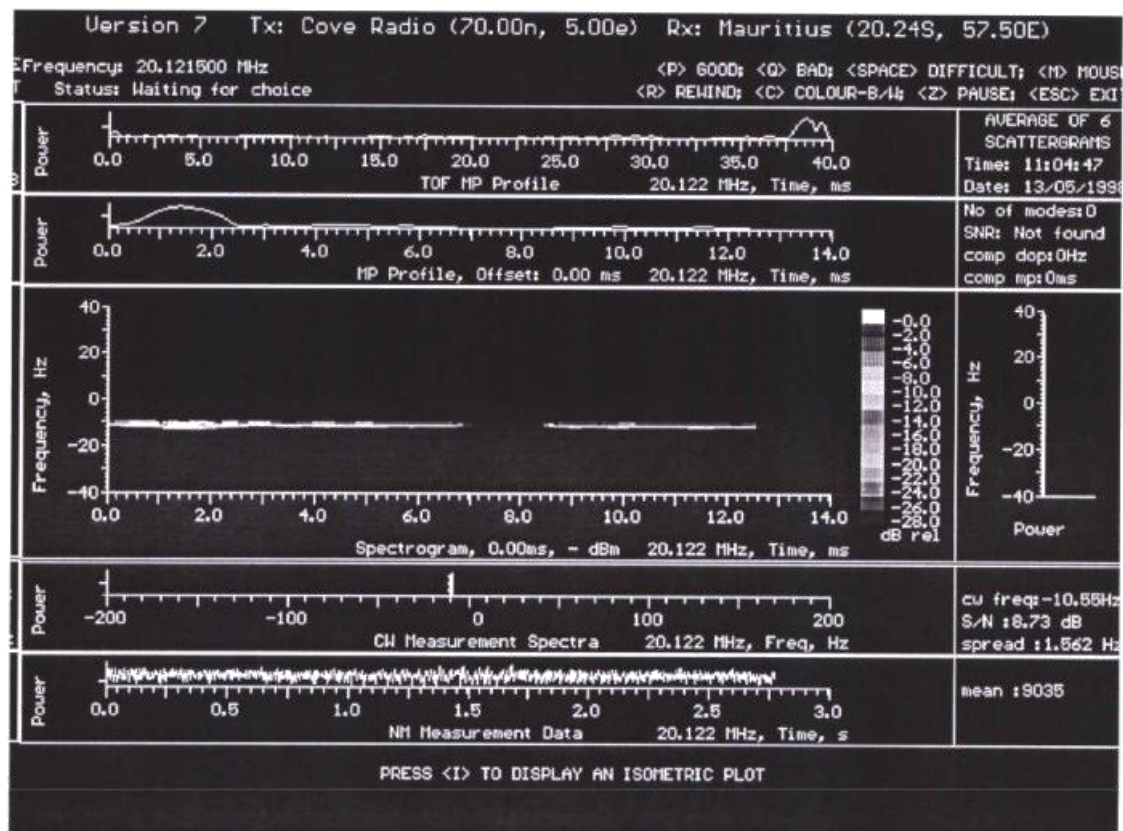


Fig. 4.9 Data from Guildford transmitting at a frequency of 20.1215 MHz

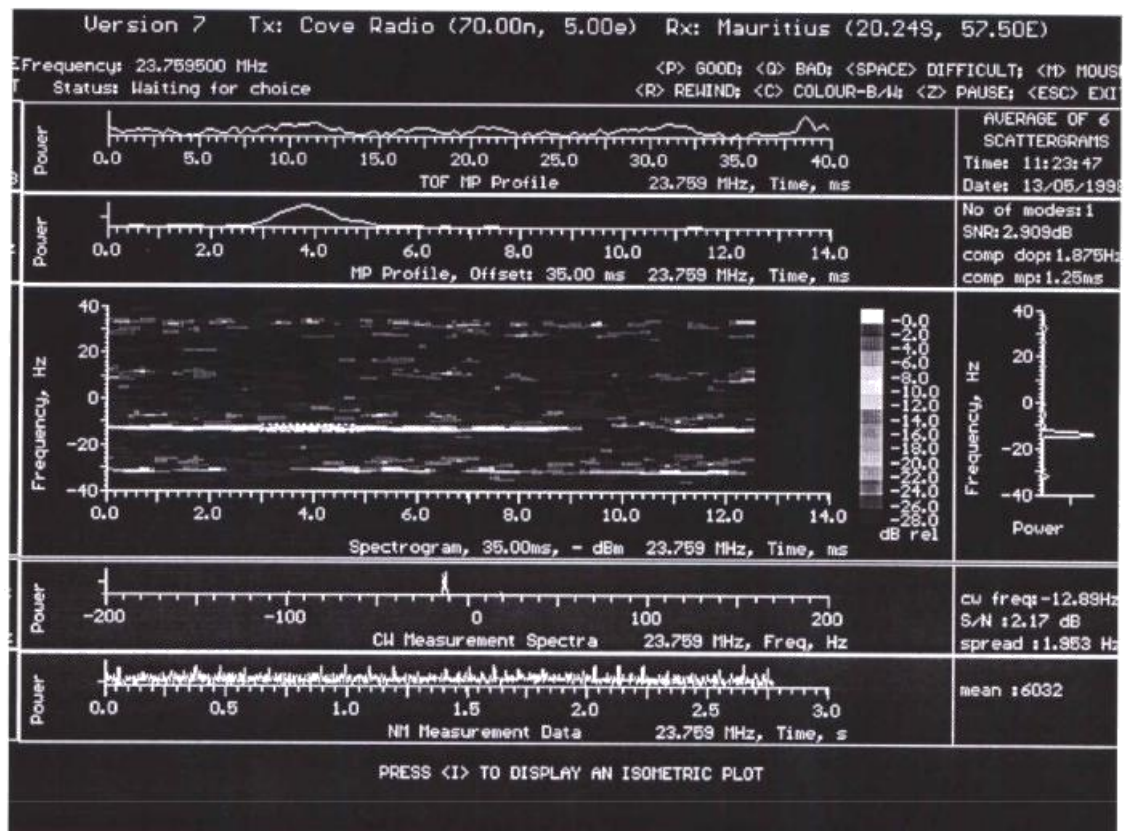


Fig. 4.10 Data from Guildford transmitting at a frequency of 23.7595 MHz

Chapter 5

Conclusion and Further Work

5.1 Summary

The research reported in this project has been carried out to determine new adaptive coding techniques applicable to time varying channels. Assessment of the performance of these codes in terms of their reliability, throughput efficiencies and burst error correcting capability has been carried out. Statistical channel evaluation based on the trellises of the linear block codes employed has been realised. Further a HF link between Europe and Mauritius has been designed and implemented. Tests carried out with data transmitted from Scandinavian and UK sources have shown that the link is working as expected. The conclusions obtained from the study including further research work are classified in the following section of this chapter.

5.2 Discussions

Embedded codes techniques [Darnell et al.1988, Darnell et al 1989, Zolghadr et al. 1988] employing hard decision decoding have been shown to give high reliability and throughput under noisy channel conditions. Embedded coding technique employing RAC and GAC codes and inner codes and outer codes has been compared with an RAC code of the same size. The performance improvement in terms of reliability and throughput efficiency have been illustrated. The outer code introduces additional redundancy and hence a scheme that does channel evaluation and error limiting by employing the trellises of the component codes has been designed and used. The disadvantage of this scheme is that different trellises are used to decode the different

components. Another embedded code has been designed that does not employ any outer codes and that employs a single trellis in a nested fashion to evaluate the channel and to decode the component codes. Each embedded code designed is seen to give improvement in terms of reliability and throughput efficiency as compared to RAC code of same block size or with a corresponding component code.

Data transmitted from Scandinavian and British transmitters have been recorded employing the receiver in Mauritius. Most of the signals received from Scandinavian sources were very noisy. However signals from Scandinavian sources were relatively good. The received mode as a hump with a time of flight just under 40 ms were clearly seen in all cases. The multipath profile showed that each of these signals are received as a single hop signal. The spectrograms gave the corresponding strength of received signals. The CW measurement in this case indicated the frequency spread is much less than 2 Hz in the case with British sources but much greater in the case of Scandinavian sources. The noise monitor averaged the noise and enabled the estimation of the corresponding SNR.

5.3 Further work

Further work will involve real time evaluation of the embedded coding techniques proposed in chapter 3 on a short term basis. However a number of other work can be carried out on a long term basis. These include

1. Efficient compression techniques applicable to HF channels.
2. Secure data transmission employing the HF channel
3. Combined coding and modulation techniques for HF channels
4. Combined source and channel coding for HF channels.

The advantages of such research will not only be the application of the HF channel, that is entirely free, for data and image transmission but all the techniques developed will be applicable to Satellite Communications as well.

5.4 Requirements

We have so far only used about Rs 100 000 from the fund allocated to us for this research. We have a receive station at the University of Mauritius. To proceed further with the project we shall need to set up a Transmit station. For this we shall need about Rs 350 000. Also we shall require about a month training in UK. This will require an additional sum of Rs 60 000. Hence a total sum of about Rs 410 000 will be required to proceed further with the project. Since We already have about Rs 390 000 left in the fund it is proposed the fund be reallocated to enable further work in this area.

Bibliography:

[Bate1992] Bate D. B.: "Adaptive coding algorithms for data transmission", Ph.D. thesis Coventry Polytechnic, February 1992.

[Bahl and Chien 1971] Bahl L.R and Chien R. T. : "Single and multiple burst error correcting of a class of cyclic product codes", IEEE Trans. Vol. IT-17 pp 594-600, Sept 1971.

[Bahl, Cocke, Jelinek, Raviv 1974] Bahl L R., Cocke F., Jelinek F., Raviv, J.: "Optimal decoding of linear codes for minimising symbol error rate", IEEE Trans. IT, 1974, 20, PP.284-287.

[Be'ery and Synders 1986] Be'ery J., Synders J. "Optimal soft decision decoders based on fast Haddamard Transform", IEEE Trans. on IT, Vol. IT-32, 1986, PP. 355-364.

[Berger and Be'ery 1993] Berger y., Be'ery y.,: " Bounds on trellis size of linear block codes' IEEE Trans. On IT, 1993, 39, (1). PP. 541-542.

[Blaum et al. 1986] Blaum M. Farrell P. G. and Van Tilborg.: "A class of Burst error correcting array codes", IEEE Trans. Vol. IT-32, pp. 836-838, Nov. 1986.

[Blaum and Farrell 1988] Blaum M., Farrell P.G.,: "Multiple burst-correcting array codes" IEEE Trans. on IT Vol. 34 PP. 1061-1066, Sept. 1988

[Brayer and Cardinale 1967] Brayer. K, Cardinale. O.,: "Evaluation of Error Correction Block Encoding For high speed HF data", IEEE Trans. Comm. Theory, Vol. Com-15, No. 3, 1967.

[Brennan 1959] Brennan D. G.,: "Linear diversity combining techniques", Proc. IRE. Vol. 47, PP 1175-1202, June 1959.

- [Burton and Weldon 1965] Burton H.O., Weldon E.J.,: "Cyclic product codes", IEEE Trans. on IT Vol- IT 11 PP. 433-439, July 1965.
- [Carvers 1972] Carvers J. K.,: "Variable rate transmission on Rayleigh fading channels" IEEE Trans. On Com. Vol. Com-20 No. 1 PP 15-22 Feb. 1972.
- [Chien 1969] Chien R.T.,: "Burst correcting codes with high speed decoding", IEEE Trans. on IT Vol-IT 15, No. 1, PP. 109-113 Jan., 1969.
- [Clark and Cain 1981] Clark & Cain: "Error-Correction coding for digital communications.", Plenum Press 1981.
- [Conway and Slone 1978] Conway J.H., Slone N.J. "Soft decision techniques for codes and lattices, including the Golay code and Leech lattice",_IEEE Trans. on IT, Vol. IT-32 No. 1, 1978 ,PP.41-50.
- [Daniel 1985] Daniel J.S.: "Synthesis and decoding of array error control codes" , Ph.D thesis, University of Manchester, UK, August 1985.
- [Daniel and Farrell 1985] Daniel, J. S.. and Farrell, P.G.,: "Burst error correcting Array codes: Further developments", 4th Int. Conf. On Digital Processing of Signals in Comm., Loughborough, UK, PP261-265, April 1985.
- [Darnell 1983] Darnell. M., : "HF system design principles" AGARD lectures series 1983, 127(Modern HF Communication), P. 8.
- [Darnell et al.1988] Darnell M., Honary B., Zolghadr F.,: "Embedded coding technique: principles and theoretical studies" IEE Proceedings Comm. Radar and Signal processing, Vol. 135, PP. 43-59, 1988.
- [Darnell et al. 1989] Darnell M., Honary B., Zolghadr F.,: "Embedded array coding for HF Channels, Theoretical and Practical studies" Proc. of IMA Conf. on Cryptography and Coding, Ed.(Beker. H.J), Oxford Univ. Press PP. 135-152, 1989.

- [Elias 1954] Elias P.: Error free coding, IEEE Trans. Vol. IT-4, PP 29-37, 1954
- [Farrell 1979] Farrell P. G.: Array codes; Algebraic coding theory and applications
Ed. G. Longo Springer Verlag PP 231-242, 1979.
- [Farrell and Hopkins 1982] Farrell P.G., Hopkins S.J.: "Burst error correcting array codes", Radio Elec. Eng. Vol. 52, No. 4, PP.188-192, April 1982.
- [Farrell et al. 1986] Farrell P.G., Honary K., Bate S.D.,: "Adaptive product codes with soft/hard decision decoding", Proc. IMA Conf. on Cryptography and Coding, Cirencester, UK 1986
- [Farrell 1990] Farrell P. G.: An introduction to array control codes, in "Geometric, codes and Cryptography". Ed. Longo, Marchi and Sgarro, Springer-Verlag, CISM No 313, 1990.
- [Farrell et al. 1991] Farrell P. G., Dunwoody V. C., Doganis N., Taleb F.: "Soft-decision decoding: A review of basic algorithms and novel techniques", 3rd Bangor communication symposium May 1991.
- [Farrell 1992] Farrell P. G.: A Survey of array control codes, European Transaction on Telecommunications and related Technologies, June 1992.
- [Forney 1988] Forney G.D., "Coset codes-part 1:Geometry and classification". IEEE Trans. on IT, Vol. IT-34 No. 5, 1988, PP.1123-1151.
- [Forney 1988] Forney G.D., "Coset codes-part 2: Binary lattices and related codes" IEEE Trans. on IT, Vol. IT-34 No., 1988, PP. 1152-1187.
- [Forney and Trott 1993] Forney G.D., Trott M.D. : "The dynamics of group codes: state spaces , trellis diagrams, and canonical encoders". IEEE Trans. on IT, Vol. IT-39, No. 5., September 1993, PP. 1491-1523.

- [Gibson 1989] Gibson J. D.,: "Principles of digital and analog communications", Macmillan publishing company, New York.
- [Goodman 1975] Goodman R.M.F.: "Variable redundancy coding for adaptive error control", Ph.D. thesis, University of Canterbury, 1975
- [Goodman and Sundberg 1984] Goodman D. J., Sundberg C. W., "The effect of channel coding on the efficiency of cellular mobile radio systems", Proc. of seminar on Digital comm., Zurich PP. 85-91 March 1984.
- [Hancock and Lindsay 1963] Hancock J. C., Lindsay W. C.: "Optimum performance of self adaptive systems operating through a Rayleigh fading medium" IEEE Trans. On Com. Systems Vol. Cs-11 PP443-453 Dec. 1963.
- [Hentinen 1974] Hentinen V. O.,: "Error performance of adaptive transmission on fading channels" IEEE Trans. On Com. Vol. Com-22, No.9 PP1331-1337 Sept. 1974
- [Honary 1981] Honary B.,: "Error correction Techniques for Bursty Channels" Ph.D. Thesis, University of Kent, 1981.
- [Honary and Farrell 1985] Honary B.K., Farrell P.G.: 'Coding techniques for HF communication systems, Proc. Fourth int. conf. On systems engineering, Coventry, Sept 1985
- [Honary and Kaya 1991] Honary B. and Kaya L.: Adaptive Array encoding Technique; Bangor Comms Symp, pp 332-336, 29-30 May 1991.
- [Honary et al. 1992] Honary B., Markarian G. S. and Darnell M.: Trellis decoding technique for array codes, Eurocode, Italy, October 1992.
- [Honary et al. 1993a] Honary B., Kaya L., Markarian G.S., Darnell M.,: "Maximum likelihood decoding of array codes with their trellis structure", IEE Proc-1 Vol. 140 No. 5, 1993 PP. 340-345.

- [Honary et al. 1993b] Honary H., Markarian G., Farrell P.,: "Generalised array codes and their trellis structure", *Electronic lett.*, 1993, 29,(6), PP. 541-542.
- [Honary and Markarian 1993c] Honary B., Markarian G.,: "Low complexity trellis decoding of Hamming codes", *Electron. lett.*, 1993, 29,(12),PP. 1114-1116.
- [Honary and Markarian 1993d]Honary B., Markarian G.,: "New simple Encoder and trellis decoder for Golay codes" *IEE Electronic Letters* Vol. 29, No. 25, December 1993, PP. 2170-2171.
- [Honary, Darnell and Vongas 1993] Honary B., Darnell M., Vongas G., : "Adaptive error control schemes for 2-200MHz multiple-mechanism propagation paths", AGARD meeting October1993.
- [Honary et al. 1995a]Honary B., Markarian G., Darnell M.,: "Low-complexity trellis decoding of linear block codes.", *IEE Proc. Commum.*, Vol 142, No. 4, 1995, PP. 201-209.
- [Honary et al. 1995b]Honary B. Soyjaudah K.M.S., Ramsawock G., Yu Wai Man Y.K.L.,: "Modified trellis decoding of simple product codes and their error performance in Gaussian channels". *Proceedings IEEE CMTC Globecom'95*, PP. 22-26.
- [Honary and Markarian 1997]Honary B., Markarian G.,: "Trellis decoding of Block codes: a practical approach", *Kluwer Academic Publishers, USA*, 1997.
- [Huber 1989] Huber K.,: "Combined Coding and Modulation using Block Codes", *Electronic Letts.*, Vol. 25, No. 7, PP. 1130-1131, August 1989.
- [Jewett and Cole 1978] Jewett W.M., Cole R.,: "Modulation and coding study for the advanced narrowband digital voice terminal", *Naval Research Lab. Report 3811*, 1978.

[Juresek et al. 1971] Jurosek. J.R., Matheson. R.J., Nesenbergs. M.,: "Interleaved block coding tests over VHF and HF channels", IEEE Trans. on Comm. Tech., Vol. Com-19, No. 5 1971.

[Kanal and Sastry 1978] Kanal L.N., Sastry A.R.K.,: "Models for channels with memory and their applications to error control", Proc. IEEE Vol. 66 No. 7, PP.724-744, July 1978

[Katakol 1987] Katakol B. S.,: "Studies on sequential decoding and adaptive techniques in communication systems via fading medium" PhD thesis IIT Kharagpur Dec. 1987.

[Kasami et al. 1993] Kasami T., Takata T, Fujiwara T., S. Lin : "On the optimum bit orders with respect to the state complexity of trellis diagrams for binary linear codes", IEEE Trans. IT, Vol. 39, No., January 1993, PP. 242-245.

[Kaya 1993c] Kaya L.,: "Trellis decoding for array codes", PhD. thesis, 1993, University of Lancaster.

[Lin and Costello 1983] Lin.S., Costello D.J.,: "Error Control Coding: Fundamentals and Applications" Prentice-Hall, NJ, 1993, PP. 458-497.

[Lin et al. 1984] Lin S., Costello D.J. Jr., Miller M. J. : "Automatic Repeat Request Error Control Schemes", IEEE comm. Mag. Dec. 1984, 22, PP 5-17.

[Macwilliam and Slone 1977] Macwilliams F. J. and Slone N. J.: The theory of error correcting codes, North-Holland 1977.

[Mandelbaum 1974] Mandelbaum D.M.,: "An adaptive feedback decoding scheme using incremental redundancy", IEEE Trans. on IT, Vol. IT-20, May 1974,PP388-389.

- [Markarian et al. 1993] Markarian G, Honary B., Soyjaudah K.M.: "Trellis decoding of adaptive product codes", Int. Symp. on Comm. Theory and Appl.. Lake District, UK, P.96, July 1993.
- [Massey 1978] Massey J., "Foundation and methods of channels encoding" Proceedings of international conference on IT 65, 18-20 Sept., 1978, Berlin
- [Matis and Modestimo 1982] Matis K.R., Modestimo J. W., : "Reduced search soft decision trellis decoding of linear block codes", IEEE Trans. March 1982, IT-28 (2), PP. 349-355.
- [Muder 1988] Muder D.J. : "Minimal trellis for block codes". IEEE Trans. on IT, Vol. IT-34, No.5, 1988, PP. 1049-1053.
- [Patel and Hong 1974] Patel A.M., Hong S.J.,: "Optimal rectangular code for high density magnetic tape", IBM jour. Res. and Dev., Vol. 18, PP. 579-588, Nov 1974.
- [Peterson and Weldon 1975] Peterson W.W., Weldon E.J.: "Error correcting codes", MIT press, Second Edition, 1975.
- [Rowland 1968] Rowland R.: "Error-detecting capabilities of two co-ordinate codes", Electronic Eng., Vol. 40, PP. 16-20, Jan. 1968
- [Shannon 1948] Shannon C.E.,: "A mathematical theory of communication" Bell Syst. Tech. Jour. 27, 1948.
- [Shannon ,Weaver 1949] Shannon C.E., Weaver W.,: ., : "A mathematical theory communication" University of Illinois Press, Urbana, Illinois 1949.
- [Shannon 1948] Shannon C.E.,: "Certain results in coding theory and control for noisy channels" Information and Control, 1, PP.6-25, Sept., 1957.
- [Sklar 1988] Sklar B., : "Digital communications: Fundamentals and applications" Prentice Hall, New Jersey, 1988.

[Slepian 1960] Slepian D. : "Some further theory of group codes", Bell Sys. Tech. Jour., PP. 1219-1252, Sept., 1960.

[Soyjaudah and Honary 1997] Soyjaudah K.M.S., Honary B.,: "Embedded code employing GAC codes and trellis decoding", 4th International symposium on Communication Theory and Applications, PP. 130-133, July 1997.

[Soyjaudah et al. 1998] Soyjaudah K.M.S., Honary B., Markarian G.,: "Phase/Frequency modulation employing REED Muller codes", Elec. Letts. Vol. 34, No. 10, PP. 957-958, May 1998

[Synders and Be'ery 1989] Synders J., Be'ery Y. "Maximum likelihood soft decoding of binary block codes and decoders for Golay codes". IEEE Trans. on IT ,Vol. IT-35, No. 5, 1989, PP. 963-975.

[Synders 1991] Synders J., "Reduced lists of error patterns for maximum likelihood soft decoding" IEEE Trans. on IT, Vol. IT-34, No. 4, 1991, PP 667-672.

[Ungerboeck 1981] Ungerboeck G.,: "Channel coding with Multilevel/phase signals" IEEE Trans. on IT, Vol. IT-28, No. 1, Jan. 1981, PP.55-67.

[Viterbi 1971] Viterbi A.J.,: "Convolutional codes and their performance in Communication systems", IEEE Trans. on Comm., Com-19, October 1971, PP. 751-772.

[Volkalis 1980] Volkalis D.C., : "A new concatenated matrix code with cluster, burst and random error correcting abilities", Int. Jour. Elec., Vol. 49, No. 5, PP.345-357, 1980

[Wolf 1965] Wolf J.K.,: " On codes derivable from the tensor product of check matrices", IEEE Trans. Inf. Theory, Vol. IT-11 PP. 281-284, April 1965

[Wolf 1978] Wolf J.K.: Efficient maximum likelihood decoding of linear block codes using a trellis, IEEE Trans. Vol. IT-24 No. 1, pp 76-80 Jan 1978.

[Yu and Lin 1981] Yu P.S. Lin S.,: "An efficient selective repeat ARQ Scheme for satellite channels and its throughput analysis", IEEE Trans. 1981 Com-29 PP. 353-363.

[Zhang and Wolf 1988] Zhang W., Wolf J.K., : "A class of binary burst error-correcting quasi-cyclic codes" IEEE Trans. IT Vol 34, PP. 463-479.

[Zolghadr et al. 1988] Zolghadr F., Darnell M., Honary B.,: "Embedded convolutional codes", Proceedings of the IERE, Firth Int. Conf. on Digital Processing of Signals in Com., 1988.

[Zolghadr 1989] Zolghadr F.,: "Embedded coding algorithms applicable to time varying channels." PhD. thesis, University of Warwick, November 1989.